Fault deformation, seismic amplitude and unsupervised fault facies analysis: Snøhvit Field, Barents Sea

University of Stavanger

Jennifer Cunningham*, Nestor Cardozo, Christopher Townsend, David Iacopini, Gard Ole Wærum

University of Stavanger

Introduction & objective

We use pre-stack depth migrated near angle stack and depth converted seismic data from the Snøhvit field, Barents Sea to complete an analysis of faults in seismic data.

The purpose of this study is to explore existing and new techniques in fault analysis to investigate the geological significance of seismic geobodies enveloping faults.

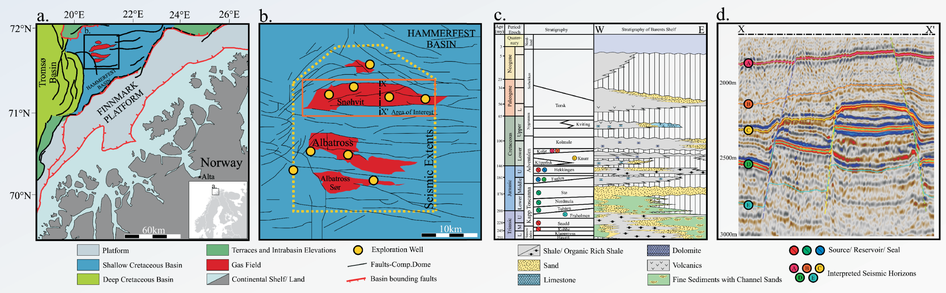

Methods & data conditioning

We integrate seismic interpretation, image processing and fault analysis methods into a single workflow designed to uncover information about 3D the geometry and internal structure of faults in seismic data.

The workflow integrates new and existing methods in seismic analysis that are commonly used in both in both industry and academia.

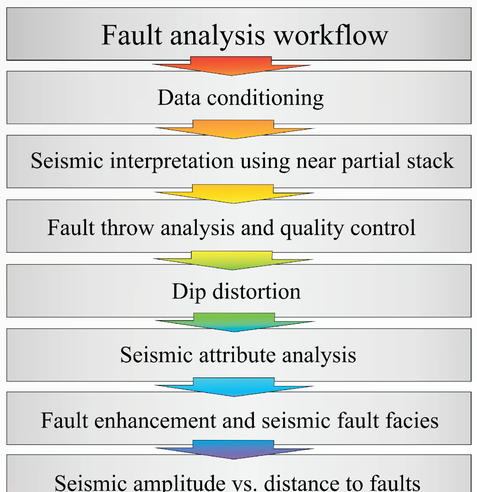

A data conditioning workflow was applied to improve signal-noise ratios and to boost seismic signal in dim areas below gas clouds in the north and west of the study area. The data conditioning was applied as below:

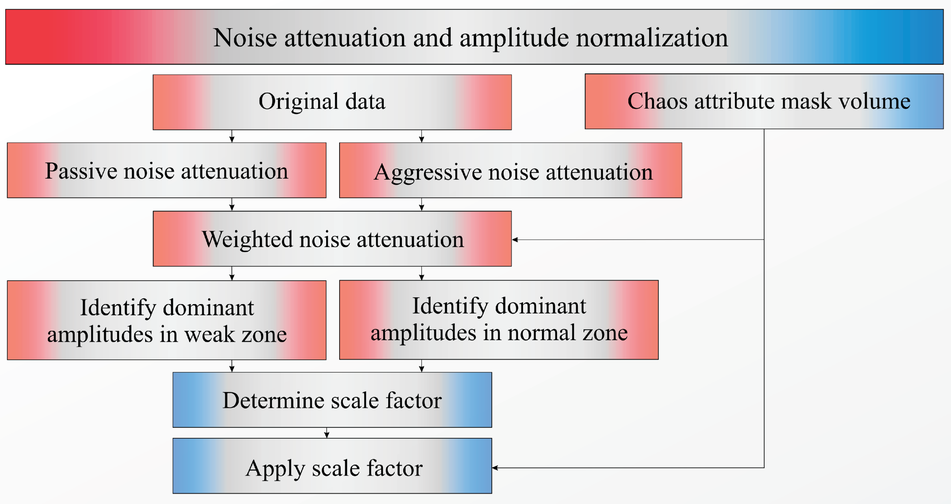

The results of data conditioning show improved seismic imaging of both seismic reflectors and faults in the study area:

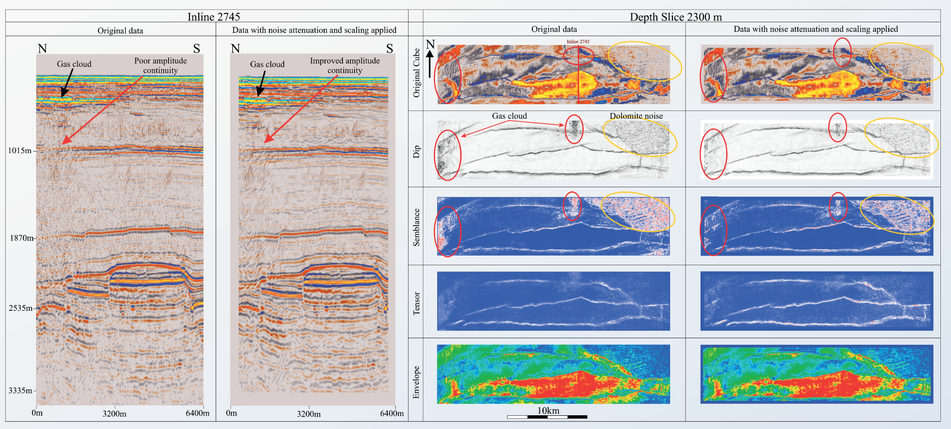

Results

Structure and thickness maps

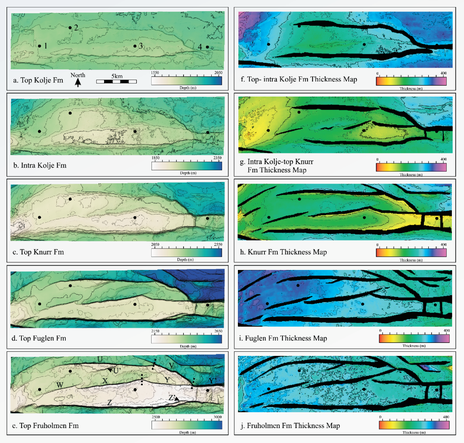

Fault throw analysis

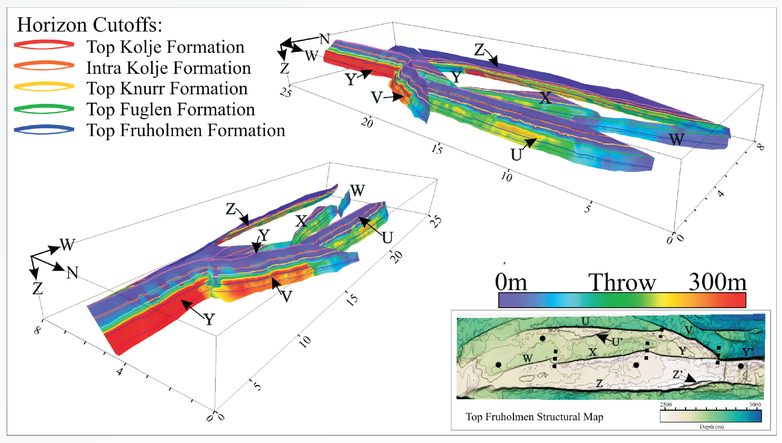

Dip distortion

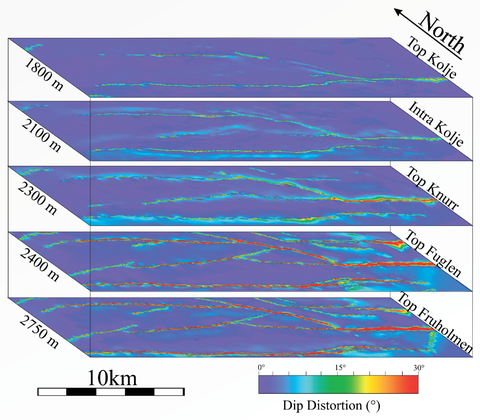

Fault enhancement and seismic fault facies

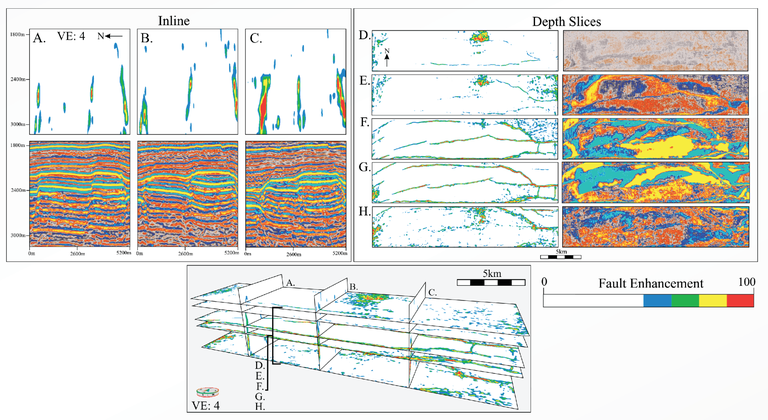

Amplitude vs distance to fault

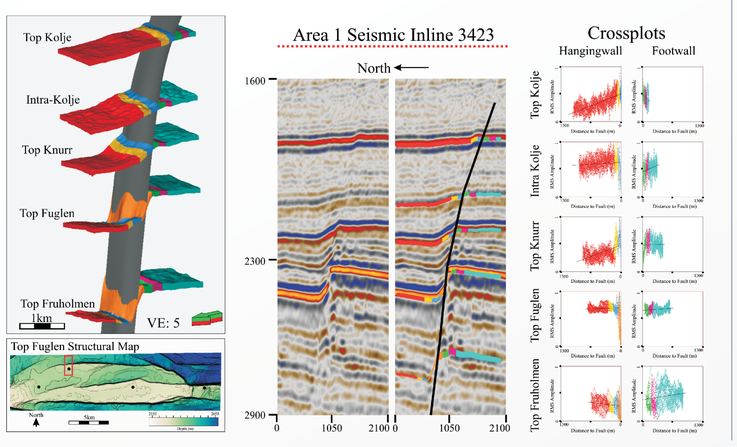

Fault facies & dip distortion comparison

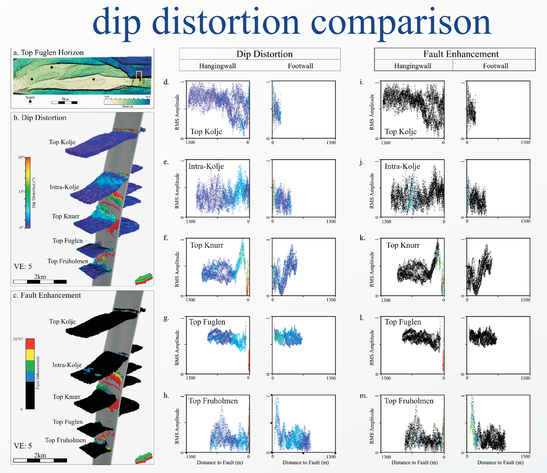

Geological comparison

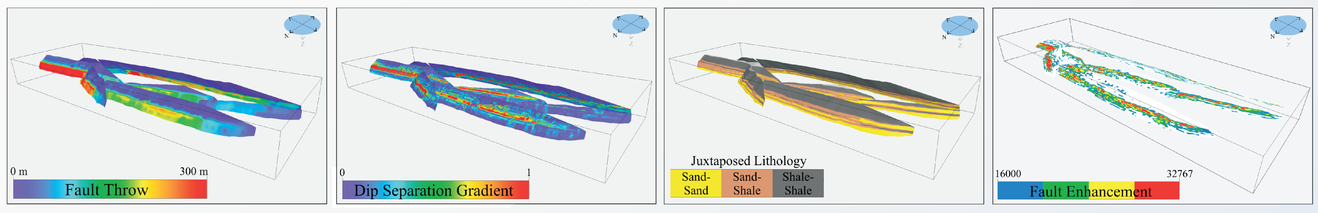

Conclusions & further work

- Workflow: Improved the interpretation and classification of seismic signal with respect to fault deformation, seismic fault facies and amplitude using industry available software.
- Dip distortion: Improved understanding of faulting, fault linkage, folding, fault tip-line, and smaller-scale faults. Identifies subtleties of folding that unsupervised seismic fault facies do not.
- Fault facies: Linked to deformation by comparing fault facies to dip distortion measurements
- Seismic amplitudes vs distance to fault: Synclines and anticlines produced a brightening or dimming in amplitude approaching the fault while amplitudes on fault planes decreased.
- Geology: Lithology, acoustic impedance, fault propagation
- Future work: An analysis of seismic data from the Snøhvit field using ocean bottom seismic data to compare how PP and PS data signals differ with respect to fault characterization.

Acknowledgments

A huge thank you to the Ministry of Education and Research in Norway for funding this research. Thanks to Equinor ASA and their partners in the Snøhvit Field, Petoro AS, Total E&P Norge AS, Neptune Energy Norge AS and Dea Norge AS who provided the seismic data for this work. We would also like to thank Schlumberger (Petrel), Geoteric (Geoteric) and Badley's Geoscience Ltd. (TrapTester) for providing us with academic licenses of their softwares.

Unraveling the depositional history of the Middle Jurassic to Lower Cretaceous succession in the SW Barents Sea

Dora Marín, Alejandro Escalona, JuLoCrA and LoCrA collaborators

University of Stavanger

Introduction

The source rock potential of Upper Jurassic rocks and the reservoir potential of Lower Cretaceous rocks is well known in the SW Barents Sea. However, the lateral and vertical variation of these rock is not well understood. Two main seismic geometries observed in the SW Barents Sea are of special interest as possible hydrocarbon targets, 1) southwards prograding and 2) clastic wedges deposited on the flanks of structural highs, as a result of a Late Jurassic to Early Cretaceous extensional event. This study integrates an extensive dataset of three and two dimensional seismic, well data and biostratigraphy to improve the knowledge of the tectonostratigraphic evolution of the southwestern Barents Sea during the Middle Jurassic to Early Cretaceous. We focused in the understanding of: 1) Sequence stratigraphy where we used stacking patterns in the GR logs to define sequences boundaries, and biostratigraphy to interpret the age of the sequences. 2) Tectonic and sedimentation and 3) paleogeography, where we use seismic interpretation, seismic facies description, attribute analysis and core description to interpret depositional environments and tectonic events that controlled the input of coarse-grained sediments to the area and the deposition and preservation of potential sources rocks.

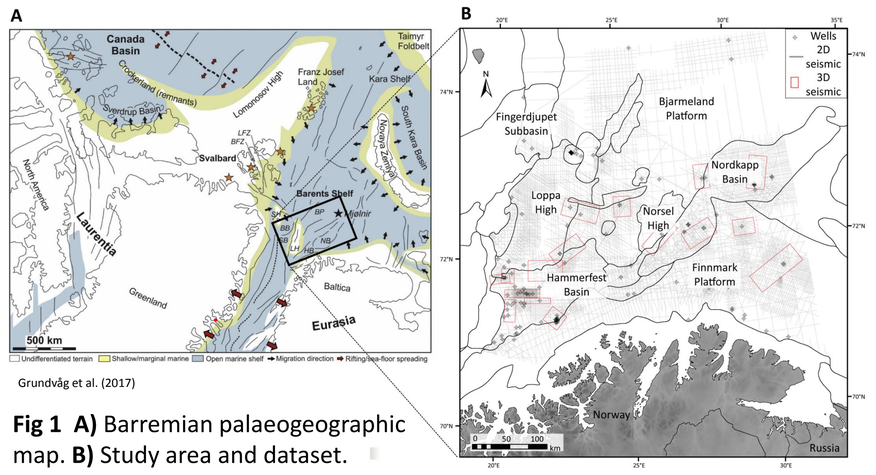

Fig 1 A) Barremian palaeogeographic map. **B)** Study area and dataset.

Sequence stratigraphy

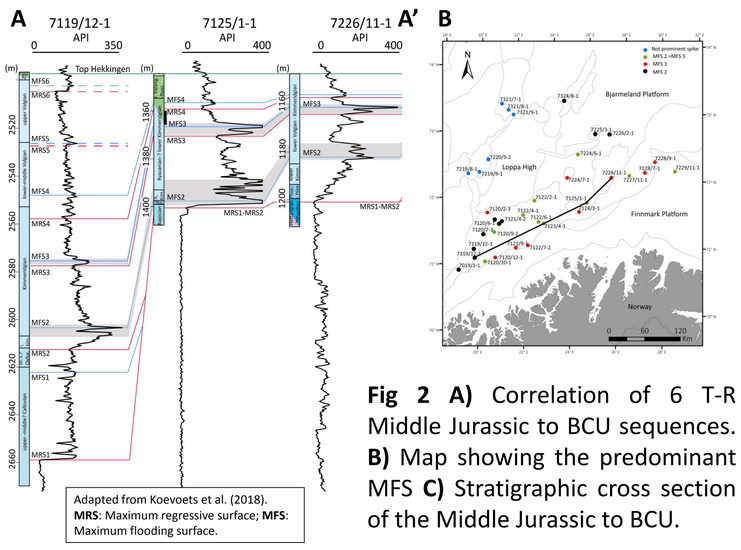

Adapted from Koevoets et al. (2018). **MRS**: Maximum regressive surface; **MFS**: Maximum flooding surface.

Fig 2 A) Correlation of 6 T-R Middle Jurassic to BCU sequences. **B)** Map showing the predominant MFS **C)** Stratigraphic cross section of the Middle Jurassic to BCU.

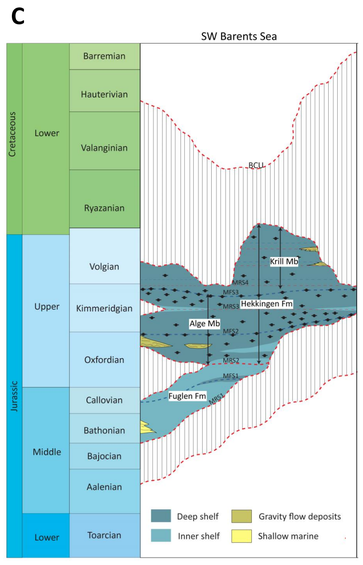

Modified from Bugge et al (2002); Grundvåg et al. (2017); and NPD (2018)

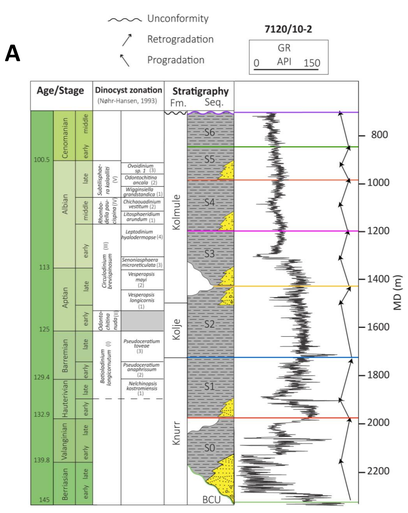

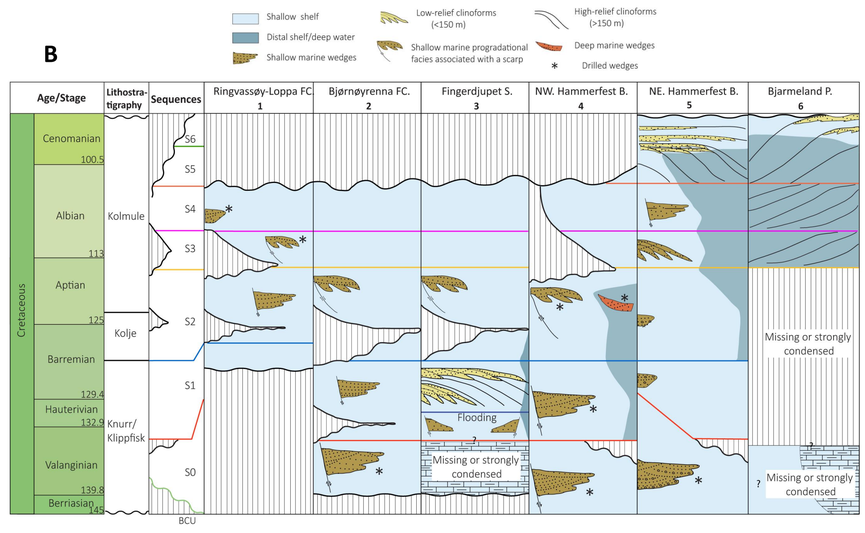

Fig 3 A) Seven Lower Cretaceous genetic sequences, provide a more robust and systematic correlation of the Lower Cretaceous wedges. **B)** Sequence correlation around the Loppa High. Note that the BCU time gap in the western flank of the Loppa High is from Late Jurassic to late early Barremian.

Tectonic and sedimentation

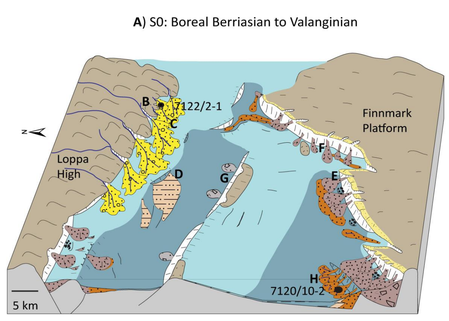

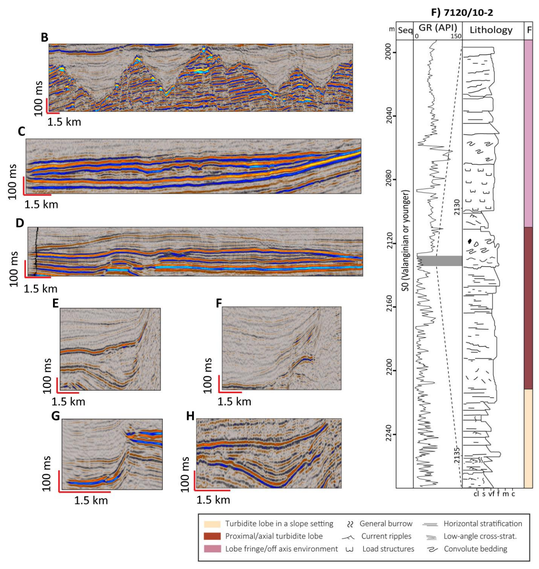

Fig 4 A) Three-dimensional paleogeographic reconstruction of the Hammerfest Basin for the Valanginian. Rift climax: Laterally continuous sandy slope systems along the southern margin. In the northern margin, a newly uplifted Loppa High provided coarse-grained sediments deposited in shallow marine environments through multiple incised valleys sources. **B-H**) Summary of the seismic facies. **F)** Sedimentary log for well 7120/10-2.

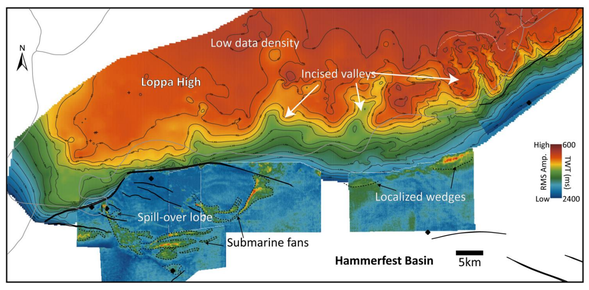

Fig 5 RMS amplitude extraction at the top of Aptian (S2) and structural map of the BCU in the northern Hammerfest basin. Submarine fans are deflected to the east. Only localized wedges are observed in the northeastern part.

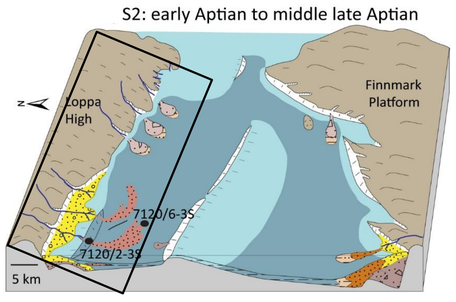

Fig 6 Three-dimensional paleogeographic reconstruction of the Hammerfest Basin for the Aptian. The input of the coarse-grained sediments was controlled by the rifting in the adjacent Tromsø Basin.

Paleogeography

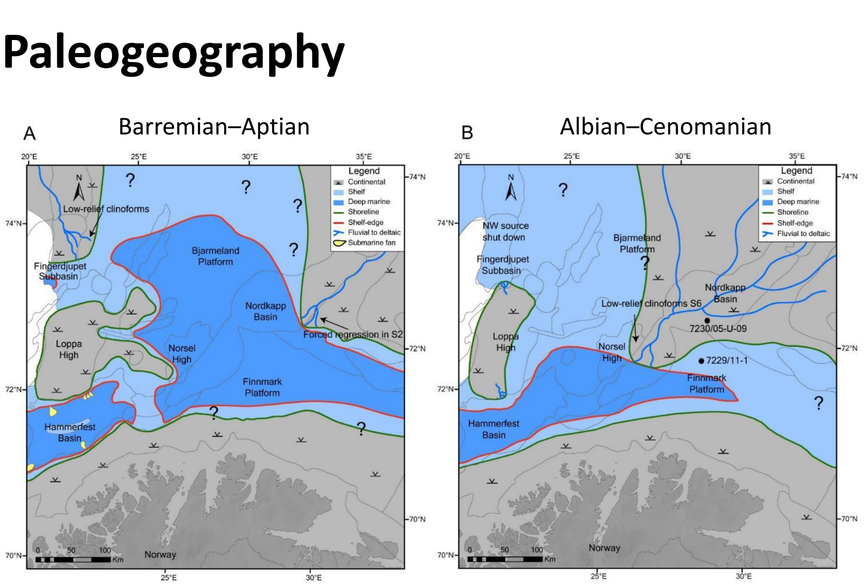

Fig 7 A) General paleogeography for the Barremian–Aptian. The shoreline represents the point of maximum progradation (during the Barremian). Areas such as the Bjarmeland Platform, Nordkapp Basin and Fingerdjupet Subbasin experienced subsequent longer term transgression. **B)** General paleogeography for the Albian–Cenomanian. Most of the Bjarmeland Platform and the Nordkapp Basin is interpreted as a shelf, where in periods of regression, deltas/shorelines could have reached the shelf-edge.

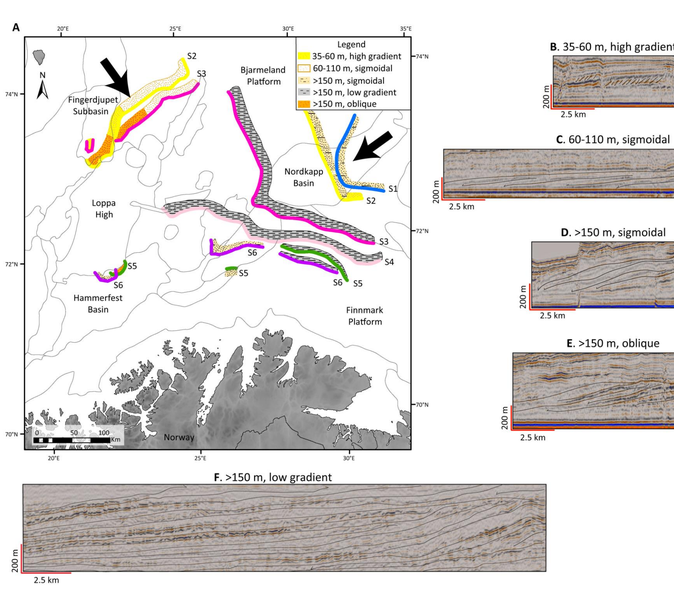

Fig 8 A) Five types of clinoform identified in the study area. **B)** Low-relief clinoforms interpreted as deltas/ shorelines. **C)** Clinoforms with a height of 60-11 m interpreted as sediments prograding in shallow waters. **D-F**) High-relief clinoforms interpreted as shelf-margin clinoforms.

Future work

1) Paleogeography and lateral and vertical variation of the Middle Jurassic to BCU succession in the SW Barents Sea.
2) Fold propagation faults and impact in the sand distribution.
3) To improve the understanding of the Upper Jurassic and Lower Cretaceous sandstones in the northern North Sea.

Publications

Marín, D. et al., 2018. Effects of adjacent fault systems on drainage patterns and evolution of uplifted rift shoulders: The Lower Cretaceous in the Loppa High, southwestern Barents Sea. Marine and Petroleum Geology 94, 212-229.

Marín, D. et al., 2018. Unravelling key controls on the rift climax to post-rift fill of marine rift basins: insights from 3D seismic analysis of the Lower Cretaceous of the Hammerfest Basin, SW Barents Sea. Basin Research 30, 587-612.

Marín, D., et al., 2017. Sequence stratigraphy and lateral variability of Lower Cretaceous clinoforms in the southwestern Barents Sea. AAPG Bulletin 101, 1487-1517

Grundvåg, S.A. et al., 2017. The Lower Cretaceous succession of the northwestern Barents Shelf: Onshore and offshore correlations. Marine and Petroleum Geology 86, 834-857.

Theoretical Comparison of Two Setups for Capillary Pressure Measurement by Centrifuge

Pål Ø. Andersen[1,2]

1 Department of Energy Resources, University of Stavanger

2 The National IOR Centre of Norway, University of Stavanger

Introduction

Capillary pressure functions can be measured using centrifuge experiments where increased rotation speed of the core forces the denser phase to be replaced by a less dense phase. In this work a modification of the conventional setup is suggested and compared with the conventional one.

Objective

- Compare the conventional two-ends-open centrifuge setup with a one-end-open setup.
- Gain understanding of the systems
- Instead of co-current displacement, the flow becomes strictly counter-current.
- What does this imply for steady state?
- How do the fluid distributions approach steady state?
- What determines the production rate?

Method

Conventional two-ends-open

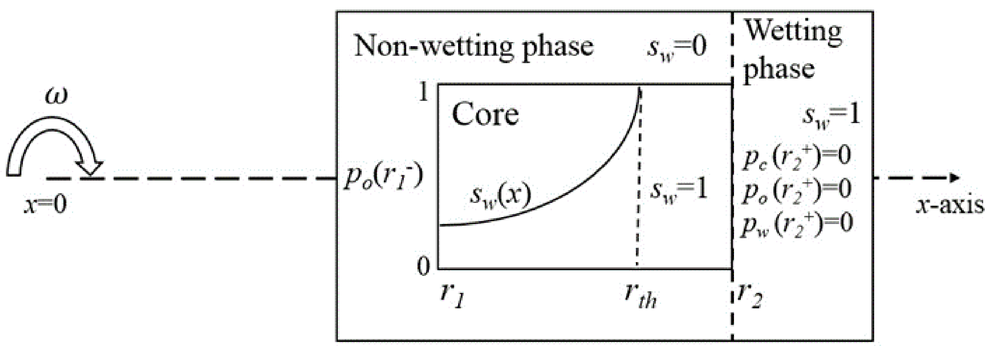

Nonlinear advection-diffusion transport equation coupled to a pressure equation:

$$\partial_t(\varphi s_w) = -\partial_x\left[\frac{\lambda_w}{\lambda_T}u_T + \frac{K\lambda_w\lambda_{nw}}{\lambda_T}\partial_x p_c + \frac{K\lambda_w\lambda_{nw}}{\lambda_T}\Delta\rho\omega^2 x\right],$$

$$\partial_x u_T = 0.$$

$$u_T = u_w + u_{nw} = -K\lambda_{nw}\partial_x p_c - K\lambda_T\partial_x p_w + K[\lambda_{nw}\rho_{nw} + \lambda_w\rho_w]\omega^2 x,$$

Velocity u_T(t) determines change in average saturation

$$\partial_t S_w = -\frac{1}{\varphi(r_2 - r_1)}u_T,$$

Modified to one-end-open

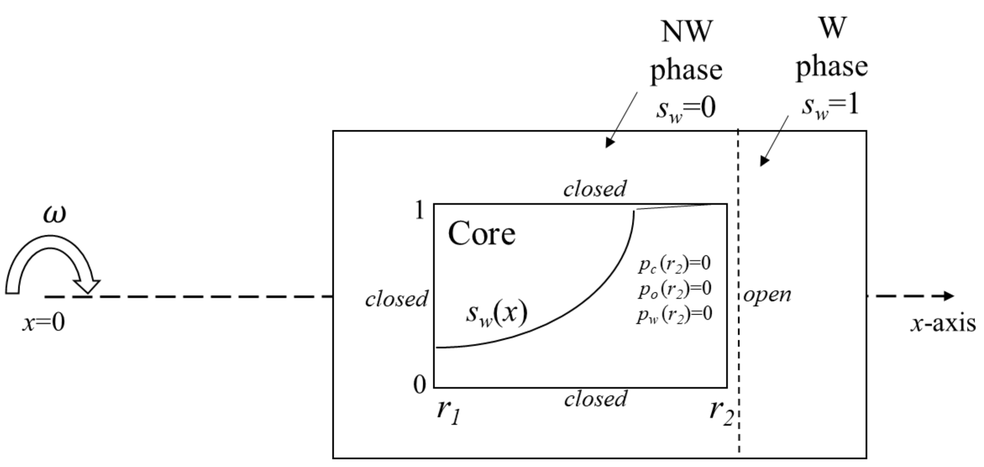

Total flux vanishes; a simpler advection-diffusion system decoupled from any pressure equation:

$$\partial_t(\varphi s_w) = -\partial_x\left[\frac{K\lambda_w\lambda_{nw}}{\lambda_T}\partial_x p_c + \frac{K\lambda_w\lambda_{nw}}{\lambda_T}\Delta\rho\omega^2 x\right]$$

Results

By setting $\partial_t s_w = 0$ and $u_T = 0$ (steady state) we get same conditions in both systems:

$$p_c^{eq}(x) = \frac{1}{2}\Delta\rho\omega^2(r_2^2 - x^2),$$

(corresponds to Hassler-Brunner condition).

Higher rotation speed increases the Pc in the core (primary drainage) and reduces wetting phase saturation (non-uniformly), see below.

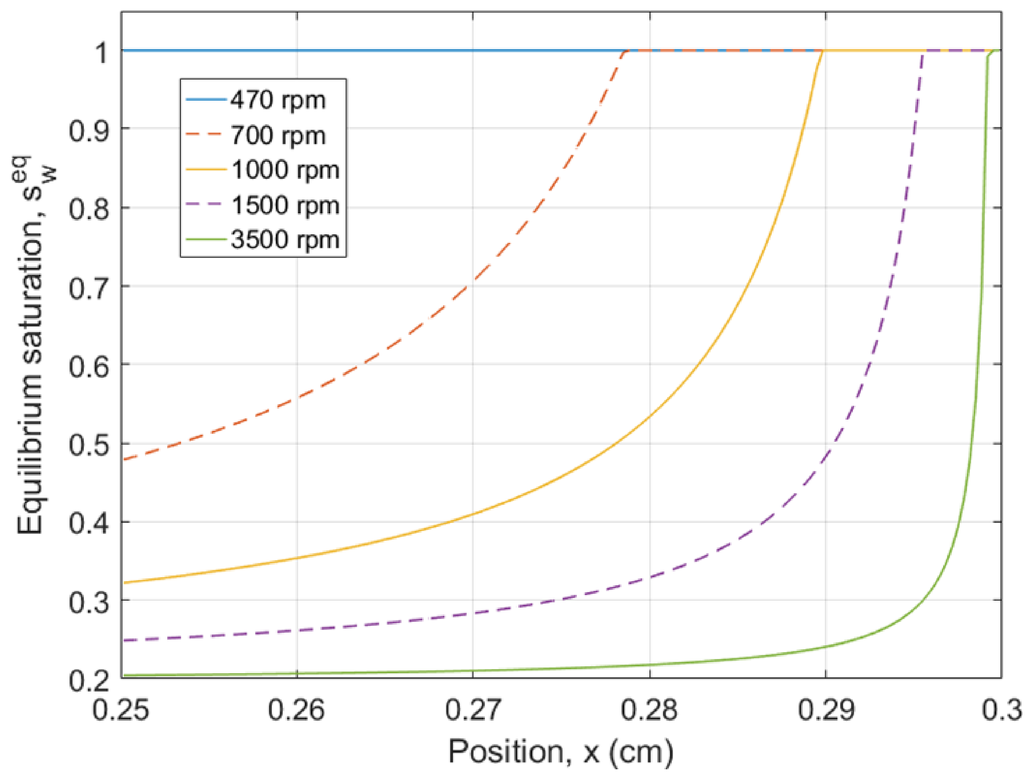

Conclusion

- Steady state can indicate flow regime dependent capillary pressure
- Transients from different flow regimes can be used to study viscous coupling and improve estimates of relative permeability
- Can better simulate conditions under counter-current gravity drainage

Further work

Most of the work is yet to be done:

- Discretization and validation of code
- Running simulations
- A comparison of these models will be presented at SPE EUROPEC 2019, London.

In future investigations more complexity will be built into the model to investigate:

- Are the flow regimes differently sensitive to viscous coupling or capillary desaturation?
- Can the methods complementary determine saturation functions more accurately?
- Can analytical solutions be constructed?

Acknowledgement

The author acknowledges the Research Council of Norway and the industry partners, ConocoPhillips Skandinavia AS, Aker BP ASA, Eni Norge AS, Total E&P Norge AS, Equinor ASA, Neptune Energy Norge AS, Lundin Norway AS, Halliburton AS, Schlumberger Norge AS, Wintershall Norge AS, and DEA Norge AS, of The National IOR Centre of Norway for support.

Scaling of recovery during immiscible WAG injection

Jan Inge Nygård[1], Pål Østebø Andersen[1,2]
[1] Department of Energy Resources, University of Stavanger
[2] The National IOR Centre of Norway, University of Stavanger

Introduction

We investigate Water-Alternating-Gas (WAG) injection in a 2D layered reservoir model and vary the influence of parameters such as mobility, gravity, heterogeneity and capillary pressure. With the increased understanding from these interactions we showcase a set of necessary conditions under which WAG injection can be recommended, and work to develop characteristic dimensionless numbers that can predict recovery trends whether one or more mechanisms are at play.

Objective

The objective of the work is to evaluate the potential for WAG injection with mechanisms such as heterogeneity, relative permeability hysteresis and capillary pressure. This is achieved using a 2D reservoir model.

Method

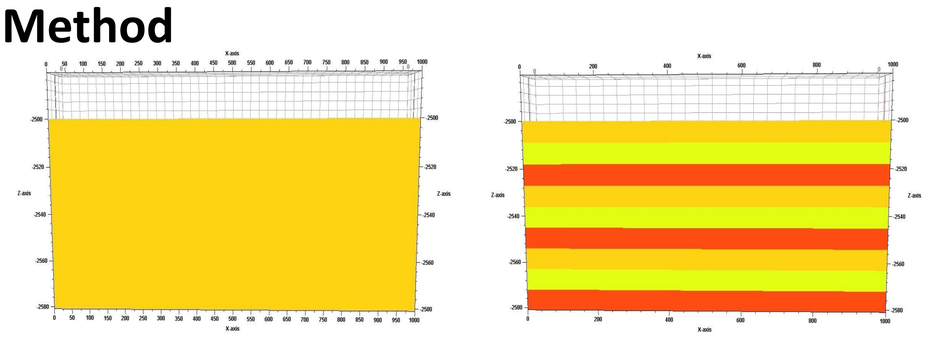

On the left: Homogeneous reservoir of 300 mD permeability. **On the right:** Heterogeneous reservoir, where layer permeability top-to-bottom consists of 300, 100, 900, 300, 100, 900, 300, 100 and 900 mD ('Base' - kx=ky=kz in each layer).

We assume Corey relative permeabilities and get the following:

$$k_{ri} = k_{ri}^{max} S_i^{n_i} \qquad S_i = \frac{s_i - s_{ir}}{1 - s_{or} - s_{wr} - s_{gr}}$$

$$M_{w/o} = \frac{\lambda_w}{\lambda_o} = \frac{\frac{k_{rw}}{\mu_w}}{\frac{k_{ro}}{\mu_o}} = \frac{\mu_o}{\mu_w}\frac{k_{rw}}{k_{ro}} = \frac{\mu_o}{\mu_w}\frac{k_{rw}^{max}}{k_{ro}^{max}}\frac{S_w^{n_w}}{(1-S_w)^{n_o}}$$

$$M_{g/o} = \frac{\lambda_g}{\lambda_o} = \frac{\frac{k_{rg}}{\mu_g}}{\frac{k_{ro}}{\mu_o}} = \frac{\mu_o}{\mu_g}\frac{k_{rg}}{k_{ro}} = \frac{\mu_o}{\mu_g}\frac{k_{rg}^{max}}{k_{ro}^{max}}\frac{S_g^{n_g}}{(1-S_g)^{n_o}}$$

$$M_{WAG} = M_{w/o}^{r_w} * M_{g/o}^{1-r_w} \qquad r_w = \frac{\text{WAG ratio}}{1+\text{WAG ratio}} \qquad \text{WAG ratio} = \frac{\text{Volume of water injected}}{\text{Volume of gas injected}}$$

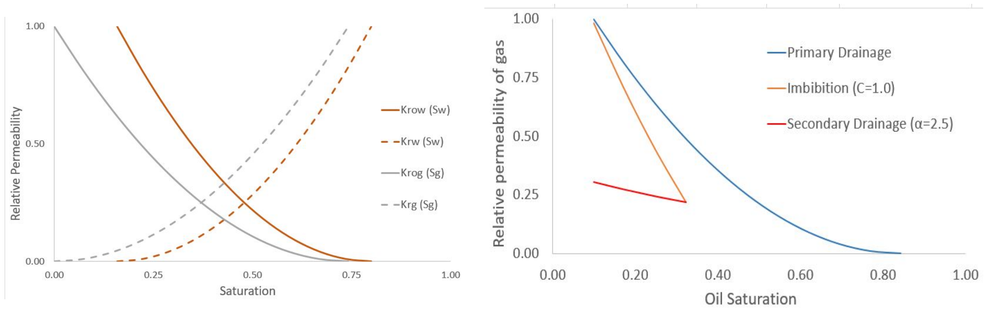

On the left: Relative permeability data. **On the right:** Illustration of the impact of hysteresis, here with C=1.0 and α=2.5, on how gas relative permeability could change.

To model the effect of relative permeability hysteresis we use the Black-Oil 'WAGHYSTR' model to simulate entrapment of gas and the consequent change in the gas relative permeability curve. We have set Land's parameter C=1.0 and the reduction factor α=2.5.

We ran a significant pool of simulations with varying degree of heterogeneity, gravity and mobility ratio to oil (Mw/o and Mg/o), where the below figures depict results from the homogeneous reservoir and which display the effect of hysteresis.

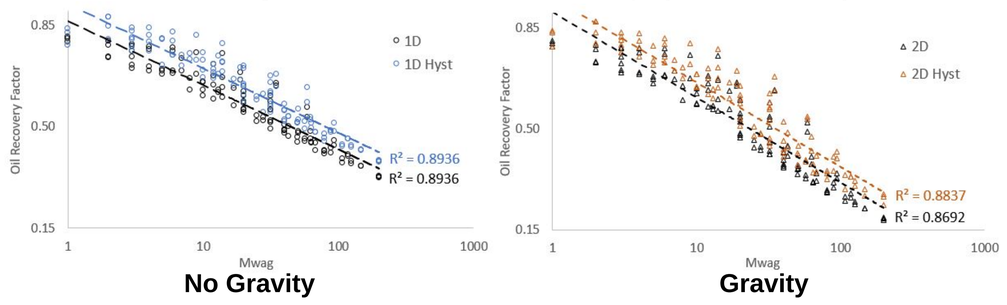

No Gravity **Gravity**

We can see that upwards of **90 % of the data can be explained with Mwag**, regardless if gravity or hysteresis is present. Similar is true for our other datasets, even with varying degree of heterogeneity and layering.

$$M_{WAG} = M_{w/o}^{r_w} * (M_{g/o} * (1 - \frac{1}{2} * C_2) * (1 - \frac{1}{2} * C_1)^{n_g})^{1-r_w} \qquad C_1 = \frac{1}{C+1} \qquad C_2 = 1 - \frac{1}{\alpha+1}$$

To capture the effect of hysteresis we developed the **above formulation**, where C is Land's parameter and α is the secondary drainage reduction factor. It is based on the fact that lower values of C and higher value of α both result in more gas trapping and a stronger relative permeability reduction. Which can be viewed as an improvement in the mobility ratio to oil, for gas.

Results

With this new formulation of Mwag we get the following corresponding figures, which captures the inherent information in the datasets and stores it in our Mwag factor instead.

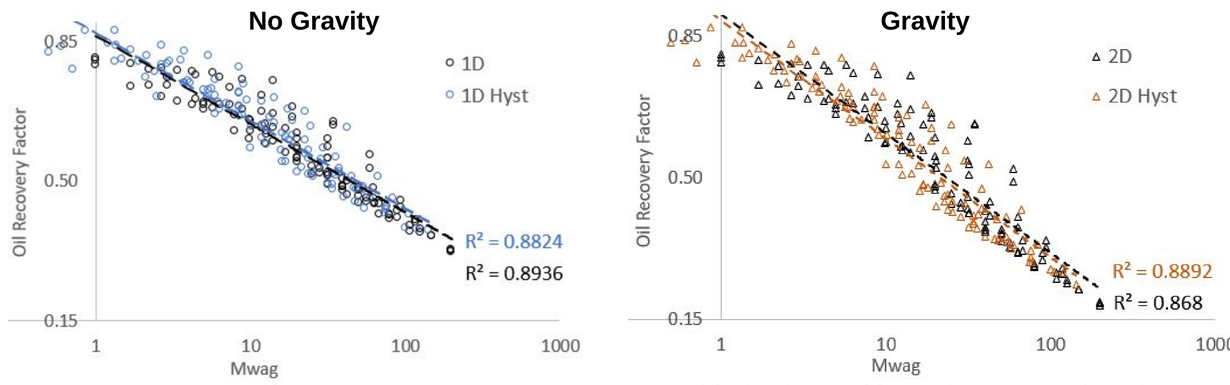

In the following we investigate the sensitivity of the model to various parameters and ask the following question: **Can WAG be recommended over single-phase injection?**

This is done with Mw/o = 20 and Mg/o = 200 to represent a realistic system where a low-mobile water phase and a high-mobile gas phase is injected.

By taking a look at all of the figures below (a-f) we can see that WAG with no hysteresis, denoted 'noHyst', never surpasses waterflood in terms of recovery. **Once we add hysteresis** to this base case, see 'Hyst', **we immediately see an improvement in WAG performance** where its recovery supercedes that of waterflood injection, which holds for all figures but a). So, yes – WAG can be recommended over single-phase injection!

Homogeneous reservoir

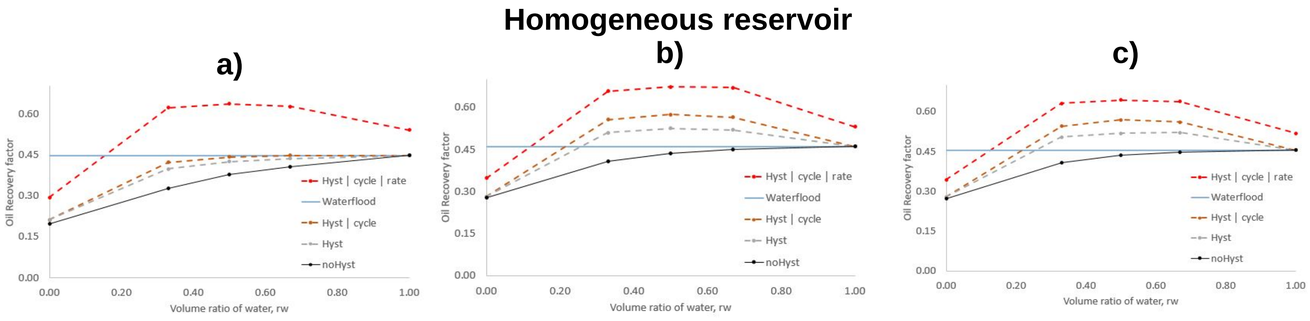

a): kx=ky=kz= 300 mD. **b):** kx=ky= 300 mD, kz= 30 mD. **c):** kx=ky=kz= 30 mD

The next step is to **double** the cycle length of WAG which means that the injected half-cycle lengths (in days) of water and gas are doubled. This effectively increases the time before which injection of water is switched to gas, and vice-versa. By comparing figures a) and b) we can see that the **reduction in vertical permeability** enabled not only the 'Hyst' case but also the 'Hyst | cycle' case to achieve a **higher recovery**. There seems to be no change going to c) and, from figures d), e) and f), there is insignificant impact of cycle length.

Heterogeneous reservoir

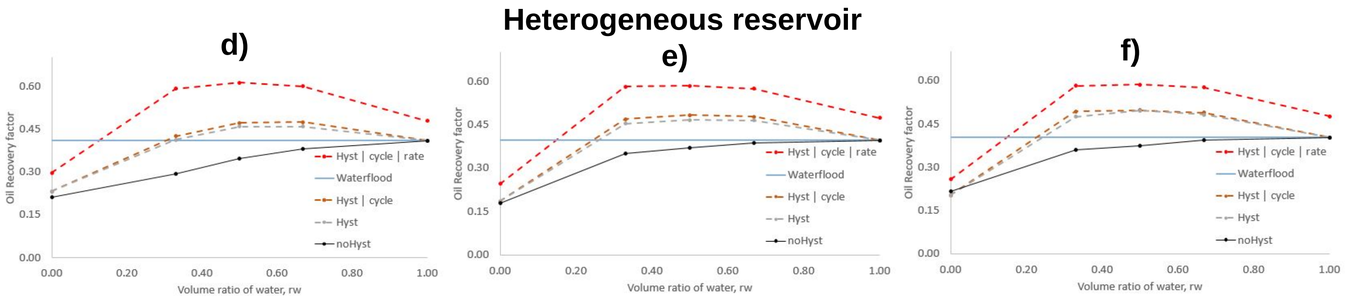

d): 'Base' reservoir. **e):** 'Base' with kz = 10 % of horizontal permeability, ie. kx=900 mD and kz=90 mD. **f):** 'Base' with kx=ky=kz in each layer but with permeabilities 30, 10, 90, 30, 10, 90, 30, 10 and 90 mD.

Moving onto **doubling** injection rate, see 'Hyst | cycle | rate', we can observe from all cases (a-f) that WAG recovery increases more than either of the single-phase injection fluids, water and gas. This is especially noticeable in a) where WAG essentially goes from being not recommended to recommended once the injection rate is high enough. This indicates that there may exist a beneficial **rate-dependency** on observed hysteretic effects, where it appears that higher rate strengthens this effect.

Conclusion

- WAG recovery can be characterized by **just one** dimensionless number, Mwag
- The viability of immiscible WAG injection depend upon the degree to which hysteretic features are present. Without them, single-phase injection is to be preferred
- This makes it important to perform laboratory measurements to evaluate gas entrapment and related hysteretic response, when evaluating the potential for WAG injection in a real field
- With hysteresis present, WAG can supercede the recovery of single-phase injection by a significant margin, even when the injected phases have vastly different mobilities.

Future work

- Extend Mwag to cover the rest of the datasets which comprises six reservoir types
- By doing so we aim to improve the understanding of WAG and build a tool which could ultimately be applied in a decision-making process.
- We are currently writing a paper to EAGE IOR 2019 on this topic

Acknowledgement

The authors acknowledge the Research Council of Norway and the industry partners, ConocoPhillips Skandinavia AS, Aker BP ASA, Eni Norge AS, Total E&P Norge AS, Equinor ASA, Neptune Energy Norge AS, Lundin Norway AS, Halliburton AS, Schlumberger Norge AS, Wintershall Norge AS, and DEA Norge AS, of The National IOR Centre of Norway for support. We also acknowledge Kenny Walrond for early contributions in setting up the model.

What is Smart Water?

Tina Puntervold and The Smart Water EOR Group

Department of Energy Resources, University of Stavanger

Introduction

Smart Water injection is a water-based EOR method aiming to improve oil recovery by wettability alteration of the reservoir from fractional wettability to more water-wet. In that process capillary forces are improved and the injected water is able to imbibe into previously unswept pores and displace the oil therein, see illustration in Figure 1.

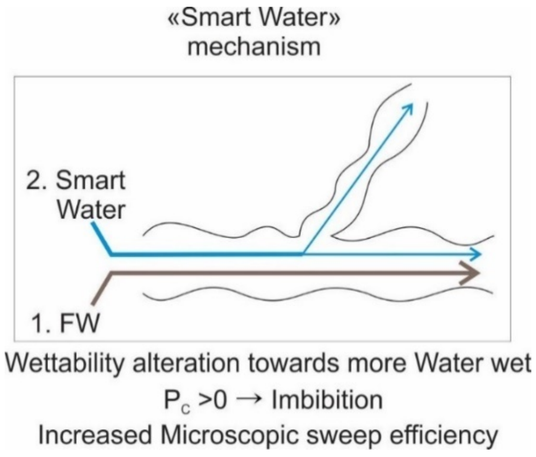

Figure 1: Increased microscopic sweep efficiency induced by wettability alteration by Smart Water injection.

Smart Water is a brine with an optimized ionic composition to alter wettability in the reservoir. No expensive chemicals, like polymers or surfactants, are added, and it is also environmentally friendly since it is based on naturally occurring waters such as seawater and fresh water.

To alter wettability, the Smart Water must interact with the reservoir minerals and the crude oil in place. Carbonate and sandstone reservoirs contain very different mineralogy, thus the Smart Water composition will be different in the two systems.

Objective

Identify Smart Water brines for carbonate and sandstone reservoirs that are able to alter wettability and enhance oil recovery by improved oil displacement.

Method

Oil recovery tests by either spontaneous imbibition or viscous flooding have been performed to evaluate wettability and the ability of different injection brines, including Smart Water, to improve oil recovery from carbonate and sandstone rocks.

Results

Seawater has been a successful injection brine in the Ekofisk field, a large chalk field on the Norwegian continental shelf. Research at the University of Stavanger has shown that seawater is a Smart Water for chalk reservoirs, due to its favorable composition containing sulfate, calcium and magnesium. It has been found that sulfate is the catalyst for the wettability alteration to take place.

However, seawater composition can be improved, by adjusting the ionic concentrations, to result in oil recovery levels beyond those obtained by seawater injection, see test results in Figure 2.

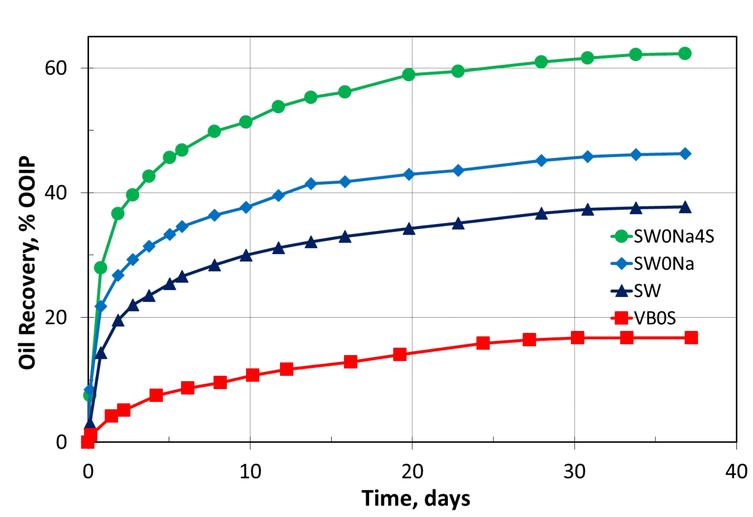

Figure 2: Oil recovery from outcrop chalk cores using different imbibition brines including formation water (VB0S), seawater (SW), modified seawater containing lower NaCl (SW0Na) and modified seawater containing lower NaCl, but higher sulfate (SW0Na4S).

In sandstone reservoirs the chemistry is completely different, therefore wettability alteration is taking place in a completely different manner, involving other minerals and ions. Thus, Smart Water composition is different. Oil recovery tests have shown that low salinity (LS) brine is a more efficient injection brine in sandstone reservoirs than a high salinity (HS) brine, or seawater (SW), figure 3.

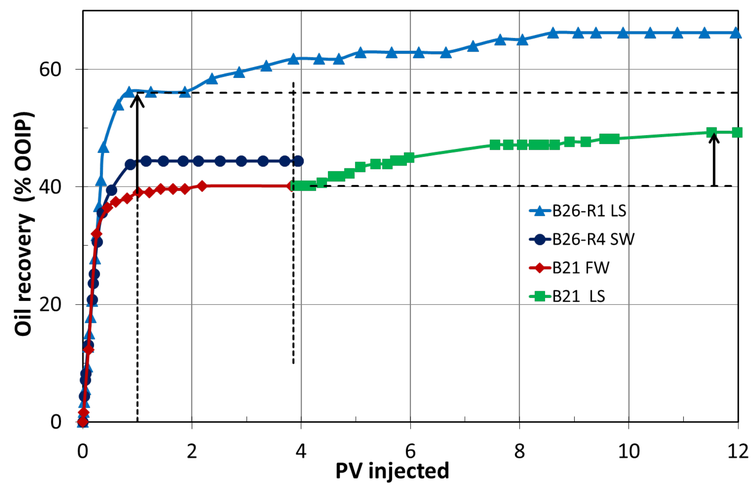

Figure 3: Oil recovery from outcrop sandstone cores using different injection brines including formation water (FW), seawater (SW) and low salinity brine (LS).

Conclusion

- Oil recovery can be improved by optimizing the ionic composition of the injected water.
- Smart Water compositions are different in carbonate and sandstone systems, due to the difference in mineralogy and the resulting reservoir chemistry.

Further work

Improving the understanding of the wettability alteration process to be able to design the best injection brine, the optimal Smart Water composition for the different reservoirs.

Acknowledgement

All students and staff who have participated in experimental work over the years, and the various companies and University of Stavanger for funding.

Reservoir chemistry controlled by mineral interaction

Tina Puntervold and The Smart Water EOR Group

Department of Energy Resources, University of Stavanger

Introduction

Smart Water injection is a water-based EOR method aiming to improve oil recovery by wettability alteration of the reservoir from fractional wettability to more water-wet. A crude oil/brine/rock (COBR) equilibrium influenced by FW composition, salinity, pH, and pressure and temperature has been established over geological time dictating the initial wettability in the reservoir. It is the polar organic components in the crude oil that is responsible for wetting the reservoir mineral surfaces, and the charges of these components are dependent on the pH of the reservoir. Thus, based on the charges, the components have different affinity to the charged mineral surfaces. Previous studies have shown that adsorption of negatively charged polar organic deprotonated acids is high in positively charged, slightly alkaline carbonate rock, while adsorption of positively charged polar organic bases is high in negatively charged, slightly acidic sandstone rock systems. In sandstone rock systems, deprotonation of polar organic components can be facilitated by increasing pH by Smart Water injection, thus altering wettability and increasing oil recovery.

The pH of the reservoir is therefore influencing the reservoir wettability. Ion exchanges at the liquid-mineral interface impact reservoir pH. Alkalinity, increased pH, can additionally be induced in-situ or even consumed by the COBR-interactions, thus affecting the EOR potential by wettability alteration.

Objective

The scope of this work is to investigate the development and transportation of pH through porous media during 1) low salinity (LS) Smart Water flooding and 2) high pH brine flooding (alkaline LS flooding)

Method

Outcrop sandstone cores were used in core flooding experiments. pH-screening tests were performed to study the pH development during waterflooding. The ability of LS and alkaline LS injection brines to increase the pH in sandstone core material was compared, and the effect of pH on oil recovery was confirmed in an oil recovery test.

Results

A Smart Water oil recovery test is presented in Fig. 1. When low salinity Smart Water was injected, a gradual increase in oil recovery was observed, reaching an ultimate recovery plateau of 49 %OOIP. At the same time, a drastic increase in produced water pH was observed, generated by cation exchange on mineral surfaces due to the ion composition of the brine.

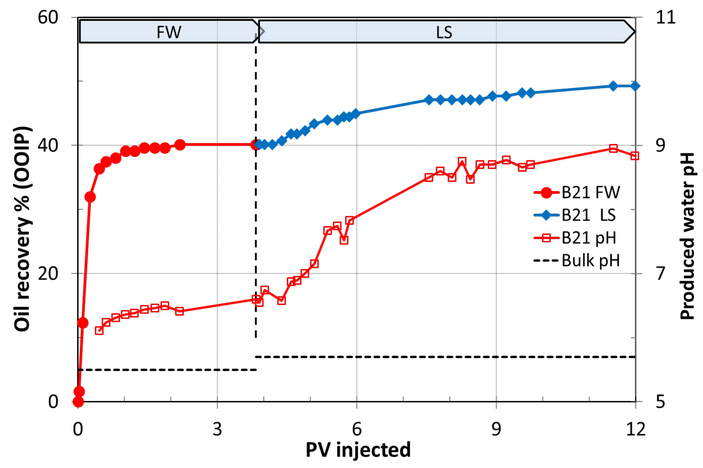

Fig. 1. Oil recovery test at 60 ° C. The core was flooded with FW-LS at 4 PV/D.

Unlike in-situ generated alkalinity by Smart Water injection, in alkaline flooding the alkalinity is attempted to be transported through the reservoir by the injection of high-pH fluids. However, reservoirs contain minerals, FW ions and crude oil components that work to neutralize the alkalinity, thus the efficiency of the alkaline flood may deteriorate. Therefore, it was of interest to study and compare the transportation of alkalinity by flooding a high-pH LS carbonate solution and LS brine through a sandstone core, Fig. 2.

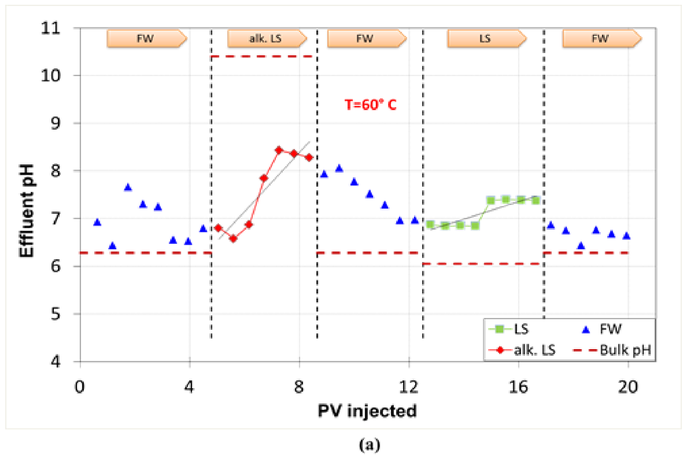

(a)

Fig. 2. Surface reactivity test performed by flooding FW, alkaline LS and LS brines through the core and measure effluent pH.

The experimental waterflooding results showed that during alkaline LS flooding the effluent pH was drastically reduced compared to the bulk pH of the alkaline LS brine. On the other hand, during LS flooding of the same core, the effluent pH drastically increased compared to the bulk pH of LS brine.

Conclusion

Cation exchange at mineral surfaces can promote or inhibit propagation of alkalinity through the porous medium. The main findings in this study were:

1. The establishment of alkaline conditions in sandstone reservoirs can contribute to an increase in oil recovery due to the creation of more favorable wetting conditions.
2. Alkalinity can be established in-situ and be transported through a porous medium by cation-exchange processes at the mineral-liquid interface.
3. A significant increase in effluent water pH was observed during LS Smart Water flooding. However, a significant reduction in effluent water pH occurred during alkaline flooding. Sandstone reservoir minerals that make up a large surface area and that control the chemical reactions in the formation caused the observed pH development.

Acknowledgement

All students and staff who have participated in experimental work over the years, and the various companies and University of Stavanger for funding.

Reservoir wettability

Aleksandr Mamonov, Tina Puntervold and Skule Strand

Department of Energy Resources, University of Stavanger

Introduction

The phenomenon of wettability describes a preference of a solid surface to be in contact with one fluid rather than another. In other words, it is a consequence of intermolecular interactions at the boundaries of phases, one of which is usually a solid and the other two are immiscible liquids or a liquid and a gas, Figure 1.

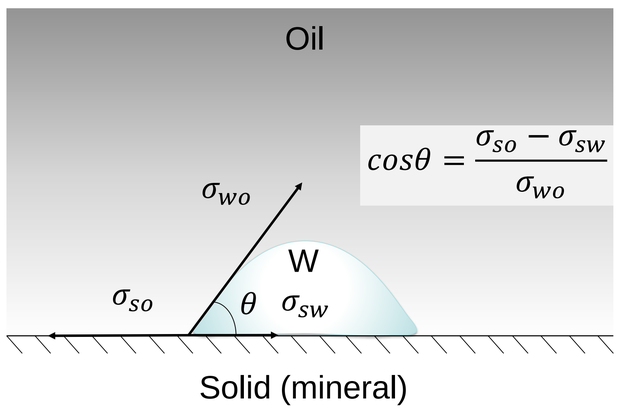

Figure 1: Wettability in the oil-water-solid system.
The wetting intensity is characterized by the magnitude of contact angle θ, which is formed by the action of forces (surface tensions, σ).

The concept of wettability of a porous medium is more complex than wetting a flat surface. In reservoir rock, the solid surface is composed of mineral grains, and the fluids in the pore space are typically an immiscible combination of water, oil and gas. In reservoir conditions the wettability is determined by the physical and chemical interactions between crude oil – brine and rocks (COBR) at the porous level. Thus, a detailed study of COBR interactions is need to be able to assess the state of the reservoir wetting, which is curtail for optimizing oil recovery.

Objectives

The primary focus of this work is on the adsorption of crude oil components onto rock mineral surfaces in sandstone and carbonate reservoirs and its effect on wettability.

Methods

The adsorption processes occurring at the interface between mineral and liquid phases in porous medium determine the reservoir wettability. The polar organic components (POC) of crude oil (acidic and basic components) can adsorb to the charged mineral surfaces if there are active adsorption centers. Thus, to study the ability of crude oil to wet mineral surfaces, core flooding adsorption tests were performed.
Crude oils with adjusted chemical compositions were flooded through sandstone and carbonate core material to compare the affinity of polar organic components (POC) to adsorb onto various mineral surfaces and change the wetting.
Adsorption of basic and acidic crude oil POC was determined by comparing the content of acids and bases in the effluent with that of the influent crude oil. Finally, the impact of crude oil components adsorption on the wettability was investigated by spontaneous imbibition oil recovery tests.

Results

Published literature ascribe wettability of reservoir rocks to the presence of asphaltenes in the crude oil, however, it was noticed that the establishment of reservoir wetting is a more complex process. The possibility of changing and recreating rock wetting conditions can be associated with the adsorption and desorption of acidic and basic polar organic components (POC) of crude oil with a lower molecular weight than asphaltenes.
Adsorption studies on chalk have confirmed that the wettability of the rock can be changed by adsorption of crude oil acids and bases not present in the asphaltenic fraction of the crude oil. Figure 2 shows an example of crude oil adsorption plot for carbonate core material and subsequent spontaneous imbibition test. POC from crude oil phase were adsorbing instantly (Figure 2a) as soon as oil was entering the core, making the chalk mineral surface less water-wet (Figure 2b). In addition, adsorption of acidic components was more pronounced than that of basic components.

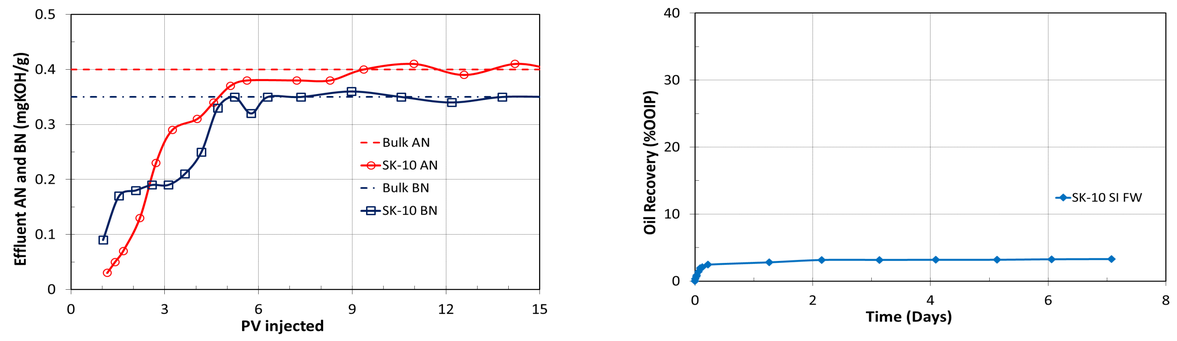

(a) (b)

Figure 2: Adsorption of crude oil acids and bases in carbonates.
(a) Acid and Base numbers of effluent oil samples. (b) Spontaneous imbibition oil recovery test.

Unlike positively charged carbonate minerals, sandstones reservoirs are mainly composed by various silicate minerals, which are normally negatively charged. Thereby, positively charged basic POC are more likely to be adsorbed onto sandstone minerals than acidic POC. This was confirmed by more pronounced BN reduction trend during crude oil adsorption test on sandstone core material (Figure 3). The amount of flooded crude oil also affected core minerals wetting sate making it less water-wet.

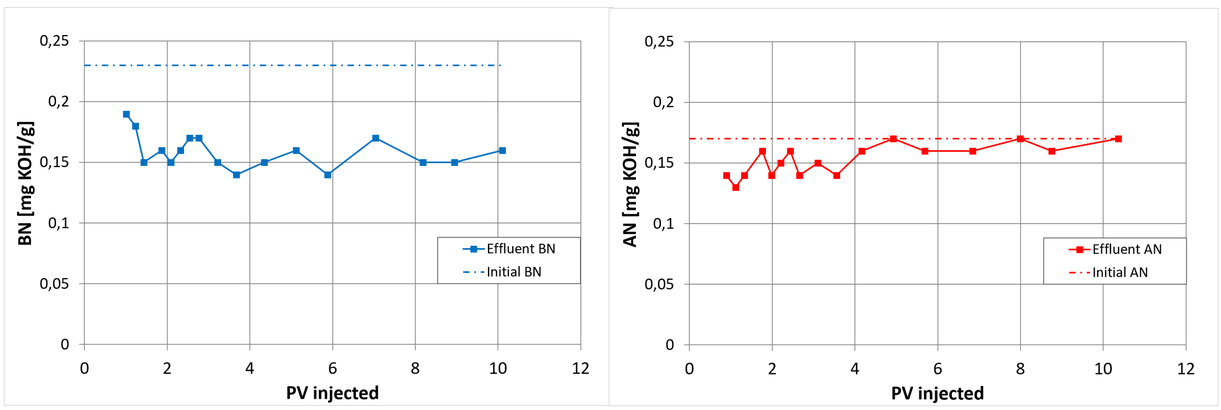

(a) (b)

Figure 3: Adsorption of crude oil acids and bases in sandstones.
(a) Base number of effluent oil samples. (b) Acid number of effluent oil samples.

Conclusions

Crude oil acidic and basic polar organic components are active towards rock mineral surfaces and can influence the wettability. Therefore, crude oil chemical composition as well as detailed rock mineralogy must be considered as an important parameters for the reliable estimation of the reservoir wettability state.

Acknowledgement

All students and staff who has participated in experimental work over the years, and the various companies and University of Stavanger for funding.

Membrane Technology for Smart Water Production

Remya Ravindran Nair, Evgenia Protasova, Skule Strand, Torleiv Bilstad

University of Stavanger, 4036, Norway

Introduction

- Nanofiltration (NF) and reverse osmosis (RO) membranes were used in this research for smart water production from seawater and oil-free produced water (PW).
- Membranes with defined pore sizes and surface charges produce required ionic composition and water recovery.
- Normal operating pressure for RO in seawater is 60 bar whereas for NF the operating pressure is 3-30 bar.

Objective

Produce smart water with defined ionic composition and flow suitable for a particular reservoir from seawater and de-oiled PW with acceptable energy consumption and without use of chemicals.

Method

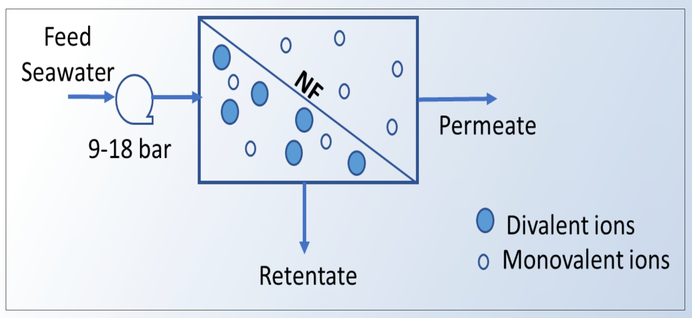

Figure 1. Schematic of smart water production from seawater

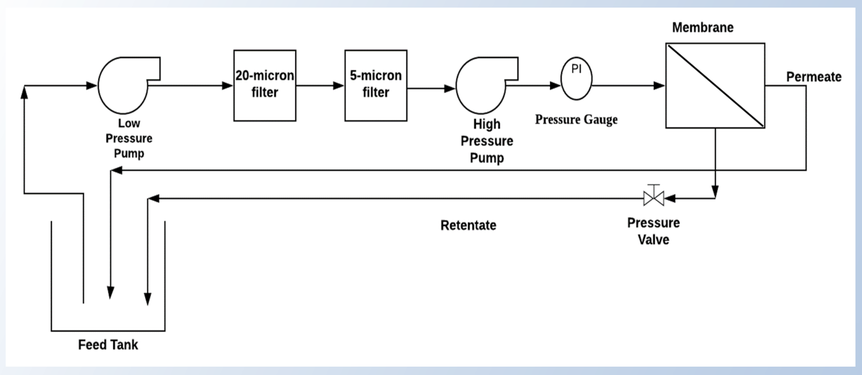

Figure 2. Schematic of membrane system used for experiments

The operating pressures were gradually changed from 9 bar to 18 bar with 25 minutes membrane stabilization time between pressure changes.

<u>Experiments with seawater as feed</u>

- Smart water for carbonates requires elevated concentrations of sulfate, calcium and magnesium. Chemicals were spiked to feed seawater to attain such smart water composition.
- No chemicals were added to seawater during smart water production for sandstone reservoirs.

<u>Experiments with PW as feed</u>

- Ba^{2+} and Sr^{2+} were removed to avoid scaling.
- TDS > 40,000 ppm for feed produced water considerably affect membrane flux. Thus, the feed was diluted before membrane separation.

Results

- Figure 3 shows that the highest rejection was for SO_4^{2-} whereas Na^+ permeated through the membrane with seawater as feed.
- Figure 4 a) shows flux variations when SO_4^{2-} concentration in the feed was increased. Figure 4 b) shows a decrease in Cl^- rejection with increasing SO_4^{2-} concentration in the feed.
- Figure 5 presents the schematics for smart water production from seawater and PW.

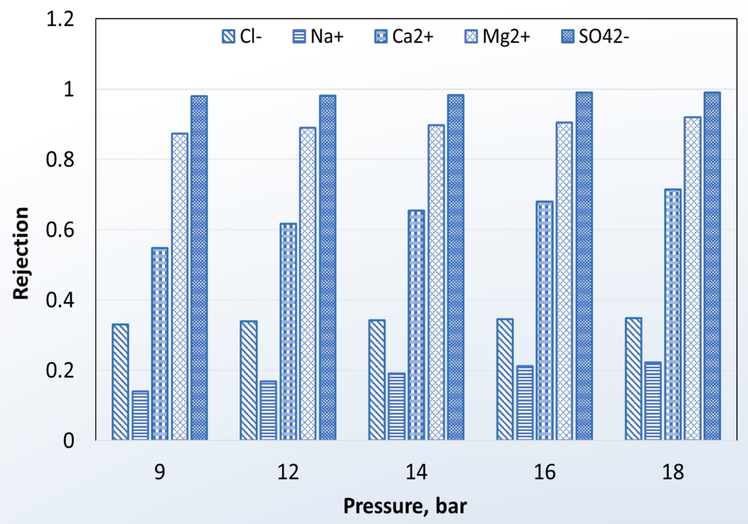

Figure 3. Ion rejection with increasing pressure

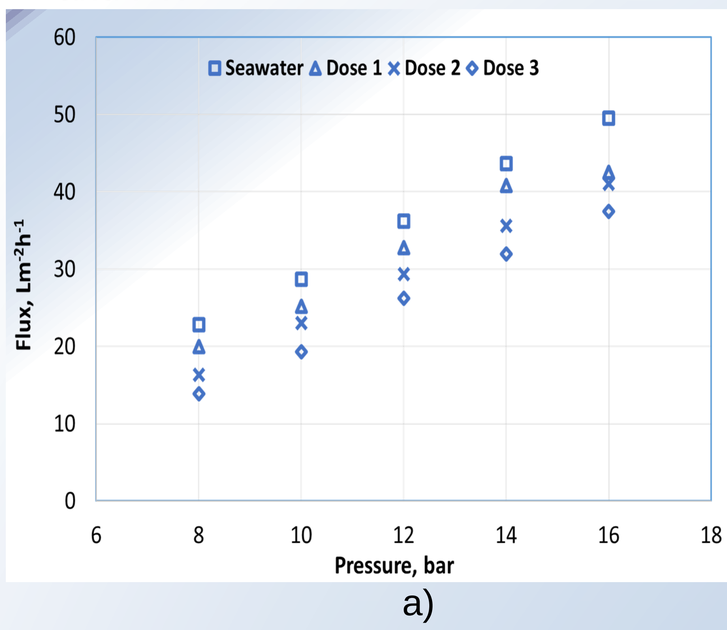

a)

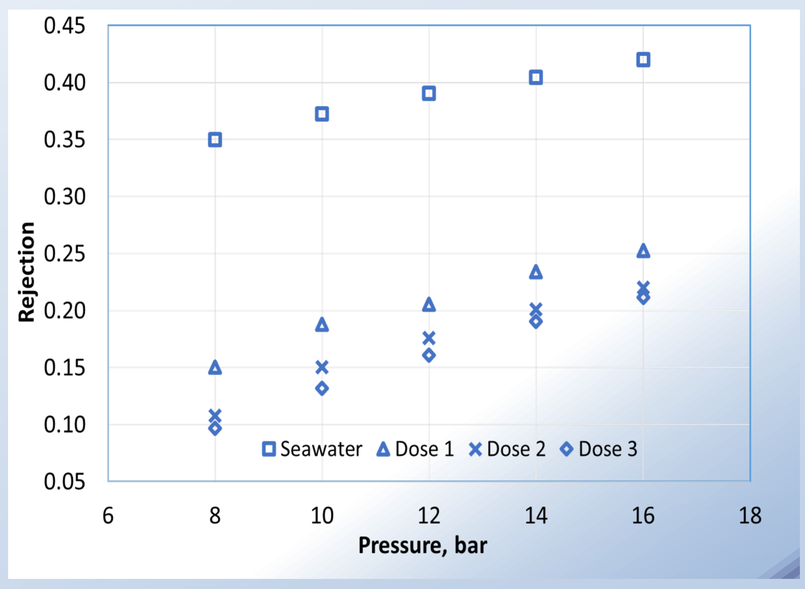

b)

Figure 4. a) Flux variations b) Cl^- rejection with increased sulfate concentration in the feed

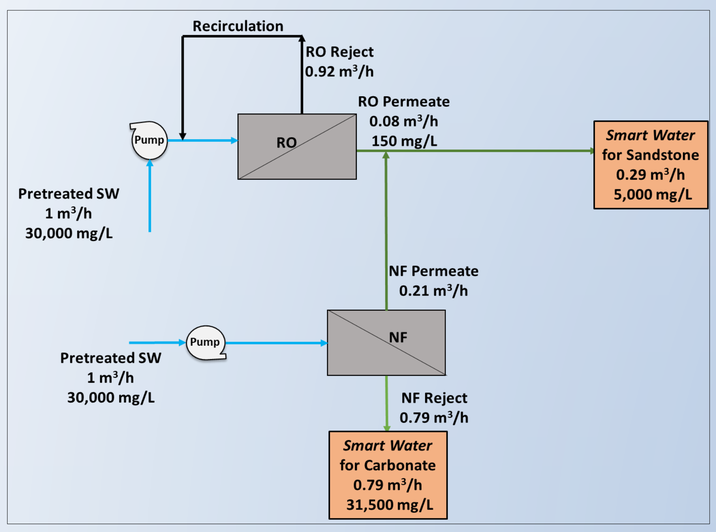

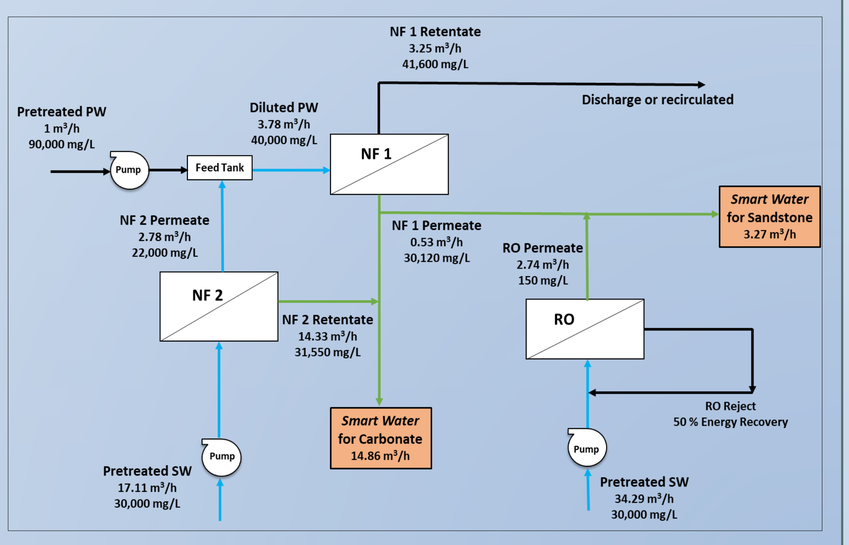

Figure 5. Schematics for smart water production from seawater and produced water

Conclusion

- Smart water rich in divalent ions or desired monovalent to divalent ion ratios, are custom made with membranes for carbonates and sandstone reservoirs.
- Flux and ion retention decreased with increasing feed concentrations.
- Power consumed for smart water production with seawater as feed:
  - For carbonates - 0.70 kWh/m^3
  - For sandstones - 5.21 kWh/m^3
- Power consumed for smart water production with produced water as feed:
  - For carbonates - 0.88 kWh/m^3
  - For sandstones - 13.99 kWh/m^3

Further Work

Core testing

Acknowledgement

The authors acknowledge the Research Council of Norway and the industry partners, ConocoPhillips Skandinavia AS, Aker BP ASA, Eni Norge AS, Total E&P Norge AS, Equinor ASA, Neptune Energy Norge AS, Lundin Norway AS, Halliburton AS, Schlumberger Norge AS, Wintershall Norge AS, and DEA Norge AS, of The National IOR Centre of Norway for support.

Initial Wetting and EOR Potential for Smart Water in Carbonate Reservoirs

Iván D. Piñerez Torrijos, Tina Puntervold and Skule Strand

Department of Energy Resources, University of Stavanger

Introduction

Smart Water wettability alteration potential in carbonates is influenced by initial reservoir wetting. Therefore, an adequate determination of reservoir wetting is crucial for a successful oil recovery operation and for the whole value of a field development plan. The initial wetting of a reservoir also sets a limit for the EOR potential during "Smart Water" injection, for this reason an improved understanding of the factors influencing the wetting can help to control and better forecast oil production during water-based floods.

Wettability alteration in carbonates with Smart Water can increase imbibition of water and at the same time, it boosts capillary action to improve microscopic sweep efficiency. The Smart Water wettability alteration in carbonates consists of a symbiotic effect among the determining ions Ca^{+2}, Mg^{2+} and SO_4^{2-} and the carboxylic material adsorbed onto the surface, the process is highly influenced by the temperature of the system.

The established chemical equilibrium of a system is disrupted by the injection of a Smart Water brine. Then, the catalyst, SO_4^{2-}, is adsorbed onto the carbonate surface. Due to this, calcium ions are able to approach the surface and displace the carboxylic material adsorbed onto the surfaces and finally altering the wettability of the surface, **Figure 1**.

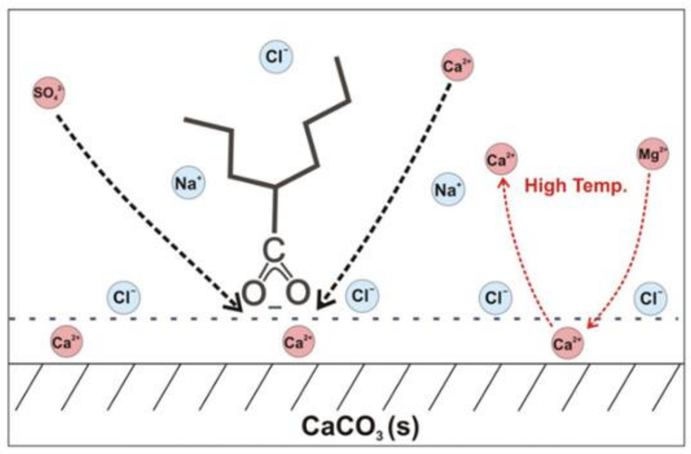

Figure 1. Description of the Smart Water mechanism in carbonates.

Objective

To gain new applicable knowledge about core cleaning and core restoration procedures. Focus will be made on components controlling initial wettability and wettability alteration processes. This will serve as a tool to design even smarter injection brines and will open new opportunities for hybrid EOR injection strategies.

Method

Parametric studies will be carried out on outcrop and reservoir material. The varying parameters to induce different wetting states will be the polar components present in the crude oil, measured by the acid and base number (AN and BN), the brine composition, and the mineralogy of the system. The initial wetting will be assessed using spontaneous imbibition and chromatographic wettability tests. Then, systematic core restoration procedures will be performed and the results will be used to validate or modify the core cleaning and restoration procedures proposed.

Results

An adequate screening routine should be run to a reliable assessment of the initial core wettability. For this reason the "Smart Water" group has developed in-house routine to adequately preserve the initial wetting of a reservoir during a core restoration procedure.

An appropriated core restoration involves cleaning of dissolvable salts, such as sulfate bearing salts that can affect wetting as described by Puntervold et al. (2008), **Figure 2.(a)**, a mild solvent cleaning associated to the organic phase is also important because it can strongly influence the wetting. Wettability should be also evaluated through spontaneous imbibition tests and further confirmed by a surface reactivity test, which was developed by Strand et al. (2006), **Figure 2 (b)**.

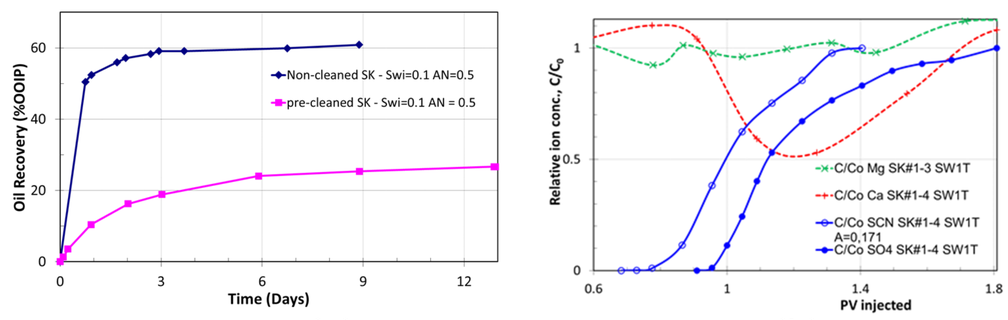

Figure 2. (a) Effect of anhydrite presence, spontaneous imbibition tests Puntervold et al. (2008). (b) Surface reactivity test example, Strand et al. (2006).

The core had a Swi ~ 0.10 established by the porous plate technique. Oil saturation was created by flooding the core with 1.5 PV of oil in each direction. The cores were aged in crude oil at 90 ° C. The restored core termed C#4 was imbibed with FW, and the oil recovery was 10% OOIP. The core was then flooded with FW, and the cumulative oil recovery reached 27.5% OOIP after 0.7 PV injected, **Figure 3**. When the flooding fluid was switched to SW, the oil recovery immediately increased to 46% OOIP after 1.3 PV injected. The injection rate was low, in the range of 0.06-0.10 PV/day, with a ΔP across the core of 4 psi at the start and 2 psi at the end. Swi ~ 0.1, and AN 1.9 mg of KOH/g.

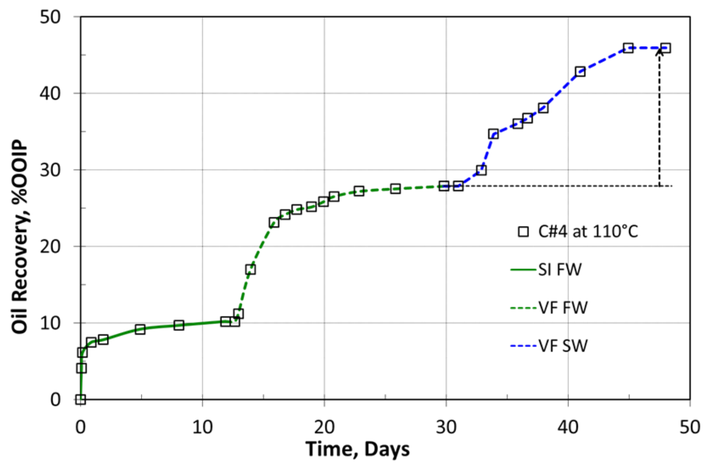

Figure 3. Oil recovery from the core C#4 at 110 ° C by successive spontaneous imbibition and forced displacement. The injection rate was in the range of 0.06-0.10 PV/day, and the ΔP across the core varied from 6 at the start to 3 psi at the end. Swi ~ 0.1, and AN) 1.9 mg of KOH/g, Puntervold et al. (2008).

Conclusions

- The restoration procedure induced slightly water wet conditions using a crude oil with an AN of 1.9 mg of KOH/g.
- Seawater induced wettability alteration with EOR effects at 110° C.
- Viscous flood was more efficient in displacing oil than spontaneous imbibition.

Further work

- Run parametric studies by changing the crude oil AN and BN, crude oil exposure and evaluating the temperature effect.

Acknowledgement

The University of Stavanger and the national IOR Centre of Norway for funding. All students and staff who has participated in experimental work over the years, and the various companies and University of Stavanger for funding.

EOR potential by Smart Water in Sandstones

Aleksandr Mamonov, Tina Puntervold and Skule Strand

Department of Energy Resources, University of Stavanger

Introduction

"Smart Water" is a modified injection brine specially designed for inducing wettability alteration to improve the oil recovery. For an optimized Smart Water design, both initial reservoir wettability and the wettability alteration need to be understood. It includes surface mineralogy, brine composition and surface-active components in the crude oil. In sandstone reservoirs, the Smart Water EOR understanding is complex, involving several chemical processes, Figure 1.

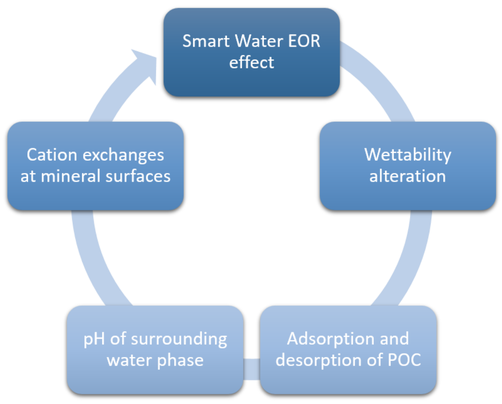

Figure 1: Smart Water EOR processes in sandstones.

A typical clastic reservoir rocks are usually composed by framework minerals such as quartz and feldspars, and also contain various clay minerals and formation fluids, Figure 2.

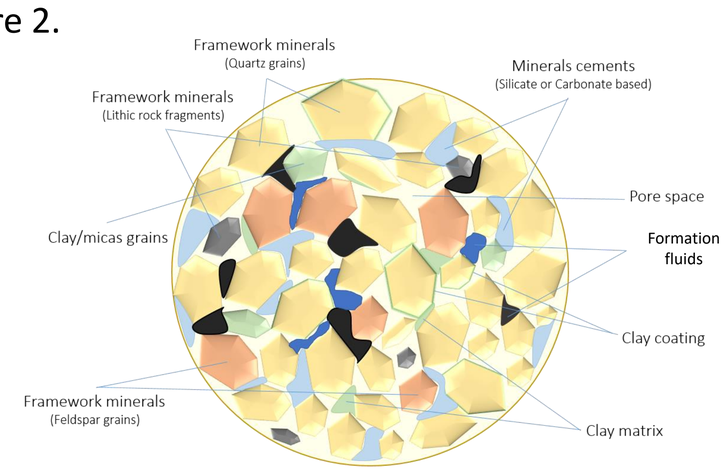

Figure 2: Schematic example of sandstone mineral structure and composition.

Each sandstone mineral has an individual reactivity towards reservoir fluids and will in its own way affect the reservoir wettability and Smart Water EOR potential.

Objectives

The scope of this work is to investigate Smart Water EOR effects in sandstone reservoirs and how different silicate minerals could affect initial rock wetting and wettability alteration during Smart Water injection.

Methods

The initial wetting and wettability alteration processes are affected by the interactions between crude oil, brines and rock minerals. The interaction between brine and rock minerals were tested by pH screening waterfloods in sandstone cores, while crude oil, brine, rock interactions were tested by static adsorption tests and core floods. Oil recovery tests were performed to compare the ability of different injection brines to enhance oil recovery from core material.

Results

Figure 3 presents an example of Smart Water EOR effects in sandstones. Figure 3 (a) shows an oil recovery test performed on outcrop sandstone core, containing all typical sandstone minerals. An increase in oil recovery is observed when formation water (FW) brine is displaced by Smart Water low salinity (LS) brine, accompanied by an increase in effluent water pH. Increased pH promotes desorption of polar organic components (POC) form mineral surfaces, which was confirmed by static adsorption/desorption studies on illite clay, Figure 3 (b). Desorption of POC shifts rock minerals wetting towards more water-wet side and that results in increase in oil recovery by improved capillary forces.

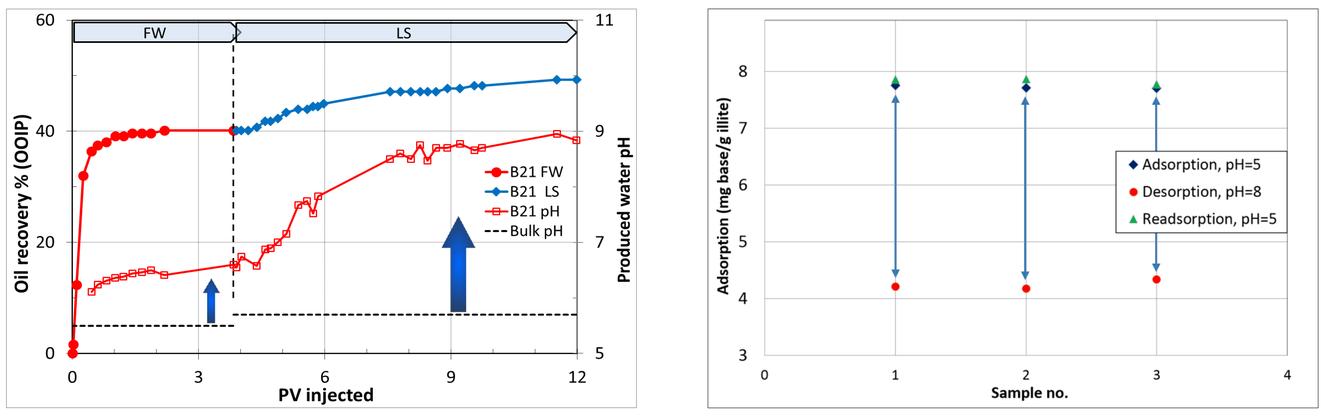

Figure 3: (a) Smart Water oil recovery test on outcrop sandstone core. (b) Static adsorption/desorption test on illite clay using Quinoline C_9H_7N as a model crude oil component.

Presence of reactive feldspar minerals may contribute to brine pH, and thereby affect the adsorption/desorption of the polar organic components. Figure 4 shows an example of pH screening test performed on feldspar rich sandstone core. In-situ alkalinity was established when FW brine was displaced by LS brine.

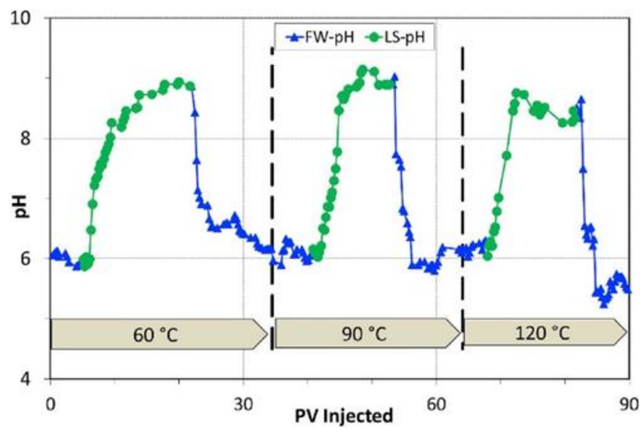

Figure 4: pH screening test on outcrop sandstone core.

Conclusions

In sandstone reservoirs, there is a potential for LS Smart Water EOR, and the underlying EOR mechanism is wettability alteration towards a more water-wet state. The wettability, in turn, is determined by the rock mineral composition and by the crude oil and FW chemistry.

Clay minerals contribute with most of the active pore surfaces, and by that influence the rock wettability state. Desorption of initially adsorbed polar organic components form the clay surface is the key reaction in the wettability alteration process. Thus, the presence of clay minerals in sandstone oil reservoirs is necessary for observing Smart Water EOR effects.

Smart Water EOR effects are generated by cation exchange and increase in pH when FW is displaced by LS Smart Water. Reactive feldspar minerals present in the reservoir rock is one of the most important factors controlling reservoir pH.

Therefore, it is important to pay attention to the reservoir mineralogy and the chemical interactions between solid and liquid phases.

Acknowledgement

All students and staff who has participated in experimental work over the years, and the various companies and University of Stavanger for funding.

Hybrid Smart Water EOR Effects

Iván D. Piñerez Torrijos, Tina Puntervold and Skule Strand

Department of Energy Resources, University of Stavanger

Introduction

Smart Water changes the rock surface wetting from mixed-wet towards more water-wet conditions, induces positive capillary forces, Pc, and improves microscopic sweep efficiency. During this process, more oil is detached from the rock surface. This redistribution of oil results in more oil trapped in the middle of the pores, due to increased capillary entrapment. Nevertheless, a fraction of this oil becomes mobile during the process. As this oil is not mobilized by water, other EOR methods can help to contact and expel the oil out of the porous media, improving macroscopic sweep efficiency, **Figure 1**.

Potential EOR methods that can be combined with "Smart Water" injection are polymer, surfactant and alkaline floods as well as water alternating gas injection, WAG, or any combination of these methods such as alkaline-surfactant, AS, alkaline-surfactant-polymer floodings, ASP.

At the same time, LS brines increase the selection of EOR chemicals like polymers and surfactants. It also increases the stability and improve the performance of these chemicals at reservoir conditions. This could improve the cost efficiency of EOR chemicals. In this work an low salinity polymer flood was implemented and termed LSP.

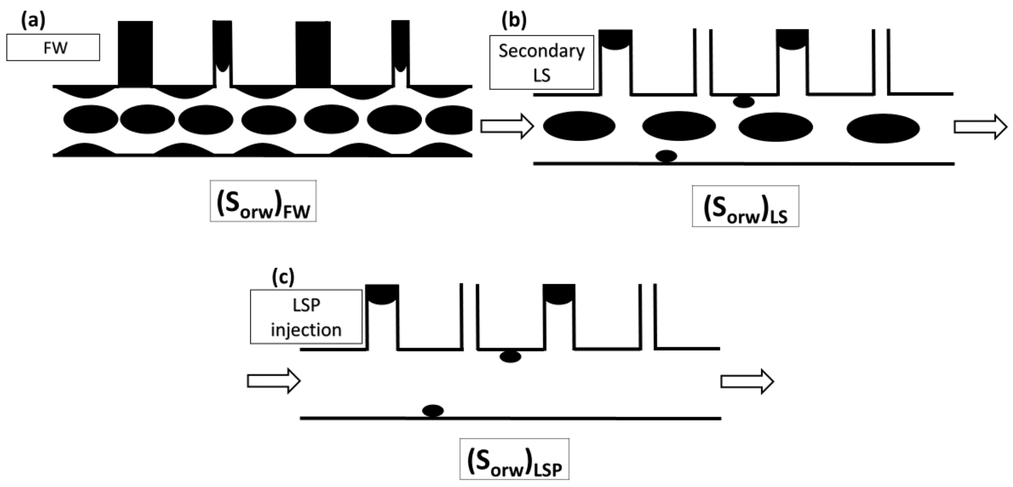

Figure 1. Mobilization of oil from a porous medium, controlled by pore size distribution and wettability alteration from mixed-wet conditions toward more water-wet conditions followed by LSP flood.

Results

The restored outcrop core B-26 was used for the Smart Water Hybrid tests, two oil recovery tests were previously performed to confirm the reproducibility of the experiment. In average, the oil recovery reached approximately a 56% of OOIP after injecting 1 PVs of the LS brine, and this was about 10% OOIP higher compared to the recovery results obtained under tertiary LS injection conditions, after injecting approximately 12 PVs, **Figure 2**.

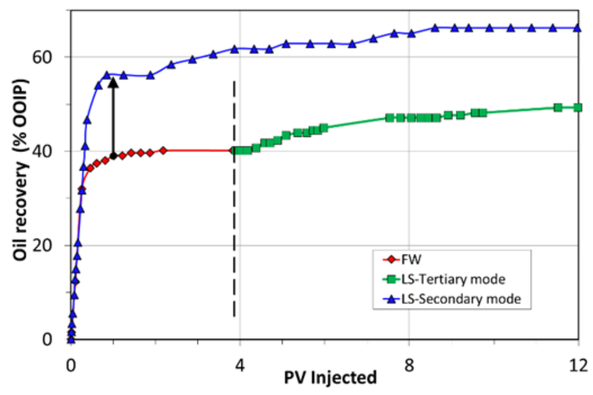

Figure 2. Comparison LS injection in secondary and tertiary mode in sandstone. Core B-21 was used to tests LS in tertiary mode, core B-26 was tested in tertiary mode. The arrow indicates the production after 1 PV injected.

In the second restoration a 1000 ppm HPAM polymer was added to the LS brine to displace the oil trapped due to increase water-wetness, the solution was named LSP. By injecting it, a fast response in oil recovery was observed, with a recovery yield close to 86% of OOIP. The response by combining LS and polymer flooding was highly efficient, improving macroscopic sweep efficiency. A possible explanation is that a part of this residual oil is perhaps trapped in the larger pores due to higher water wetness after the LS flood. However, the most important is that the trapped oil is easily mobilized by the injected LSP solution, **Figure 3**.

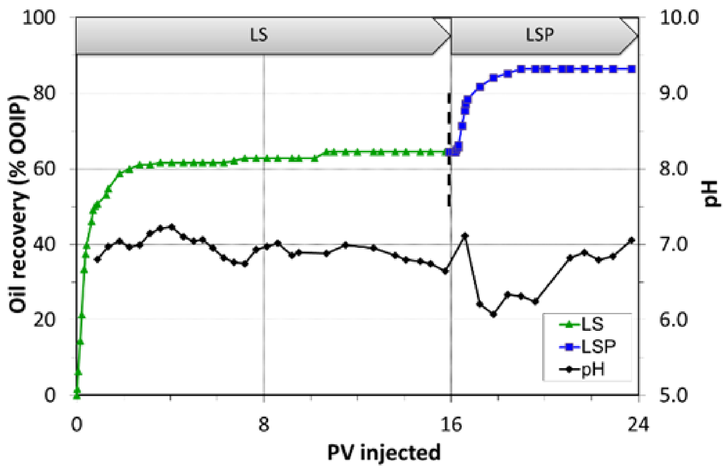

Figure 3. Oil recovery test from core B-26 at 60 ° C by secondary injection of LS brine. Second restoration of core B-26 after mild cleaning with LS in secondary mode followed by a LSP flood (right).

Objective

To evaluate the benefits of using Smart Water in hybrid EOR processes in sandstone reservoirs and characterize the EOR effects observed.

Method

An oil recovery test by viscous flooding was performed on a restored core. The restored core was mounted in the core holder with a back pressure and confining pressure of 10 and 20 bar respectively. The core was successively flooded with low salinity brine, **LS**, flowed by a low salinity polymeric solution, **LSP** at constant rate. The cumulative oil produced was monitored, as well as pH and salinity of the produced water.

Conclusions

- A fast oil recovery of approximately 56 % of OOIP after injecting 1 PV which was about 10% OOIP higher than the recovery at tertiary LS flooding conditions at the same injected PV. The total oil recovery approached 64% OOIP after 8PVs.
- In addition to this, a tertiary LSP flood was performed and a fast response in oil recovery was observed.
- The ultimate oil recovery was in the range of 86% of OOIP. This means that due to the change in wetting by the LS flood a significant fraction of oil was trapped by a snapped off process, but the polymer was able to contact it and expel it from the porous media increasing drastically oil recovery.

Further work

- To test Smart Water with other chemical EOR methods such as WAG, surfactant flooding or other type of surfactants.

Acknowledgement

TOTAL E&P, the University of Stavanger and the national IOR Centre of Norway for funding. Special thanks to the students Hakar Ihsan Abdullah and Tord Hanssen Bleivik for their contribution with experimental work.

Ongoing research activities on Smart Water EOR

Tina Puntervold and Skule Strand

Department of Energy Resources, University of Stavanger

Introduction

Smart Water significantly improves oil recovery in both Carbonate and Sandstone reservoirs. Wettability alteration from fractional towards more water wet conditions are experimentally confirmed by spontaneous imbibition (SI).

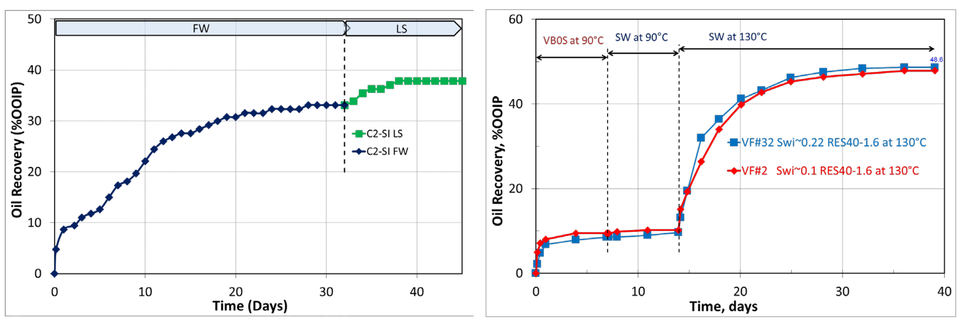

Figure 1: SI experiments confirms wettability alteration (left) with LS brine in Sandstone and (right) with SW in Carbonate (chalk.

Positive capillary forces are increased and the brine imbibes into non accessible/unswept pores and displace/mobilize oil. Smart Water is a brine with optimized ionic composition, and are environmentally friendly since it is based on naturally occurring waters such as seawater and fresh water. Core experiments on real reservoir systems confirms significant increased oil recoveries.

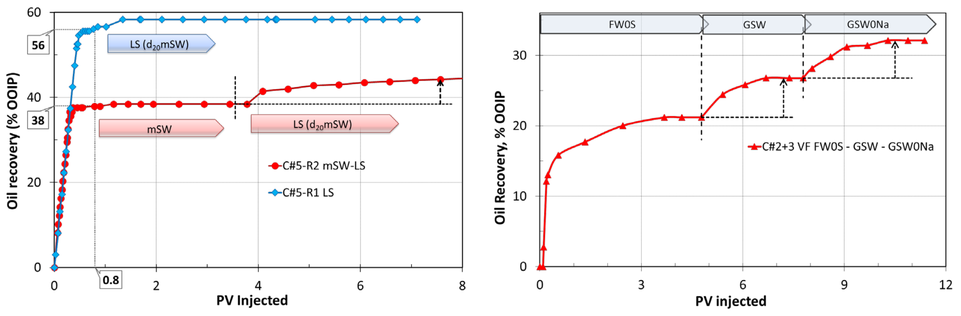

Figure 2: Core flooding experiments on restored reservoir cores confirming significant Smart Water EOR effects in (left) LS injection in sandstone, and (right) SW and modified SW injection Limestone.

Objective

Reservoirs consists of 3 main phases, Minerals, Brine and Crude Oil (CoBR). The objective is to identify all main reservoir parameters that dictates reservoir wettability and the conditions needed to induce wettability alteration within the time frame of reservoir production.

Method

Carbonate and sandstone reservoirs are very different in mineralogy. The pore surface minerals and the interaction between surface active components in FW and Crude oils components dictates reservoir wettability. Wettability alteration processes are also controlled by the same chemistry.

The chemical reactivity of reservoir minerals need to be known to predict reservoir wettability, and also to be able to predict the Smart Water EOR potential. Chemical induced adsorption and desorption studies are performed on mineral surfaces in batch systems, in sand pack experiments, and in outcrop and reservoir cores. Adsorption of polar organic components are measured, and SI experiments performed to verify changes wettability.

Experimental verified results are used to develop chemical and physical models for describing wettability dependent fluid flow in porous media.

Oil reservoirs consists of 3 main phases, Minerals, Brine and Crude Oil (CoBR).

Crude Oil	Brine	Rock
• Polar organic acids • Polar organic bases	• Formation Water salinity and Ion composition • Injection Water salinity and Ion composition	• Carbonate • Sandstone • Mineral surface reactions • Mineral dissolution

In classical reservoir engineering only physical parameters are included when fluid flow in porous media are described, and further modelled.

Research activities in the Smart Water EOR group :

- o Carbonate and Sandstone reservoirs
- o Develop increased competence and knowledge of:
  - Pore surface mineralogy
  - FW composition
  - Crude oil properties
- o Pore heterogeneity
- o Initial wettability
- o Core restoration procedures
- o Wettability alteration - Smart Water EOR processes
- o Chemical and physical models describing EOR mechanisms
- o Optimized injected water composition to maximize oil recovery.
- o **Prediction tools to evaluate Smart Water EOR potential for given reservoirs**
- o Injection strategies combining Smart Water EOR with other EOR techniques
  - WAG
  - Polymer
  - Surfactants
  - Alkaline flooding

Fluid flow in heterogeneous porous media:

- o Controlled by capillary forces

Wettability alteration with Smart Water induces:

- o Increased capillary forces
  - More stable displacement front
- o Redistribution of oil
  - Unstick oil from pore surfaces
  - Reduced immobile residual oil

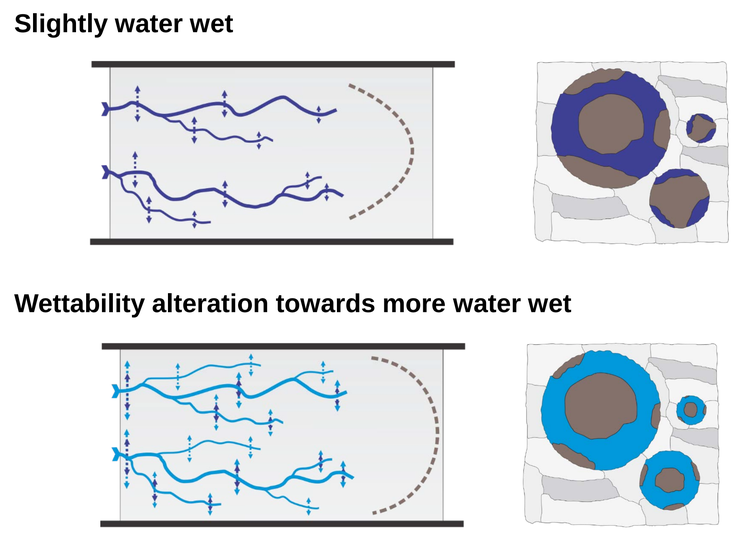

Figure 3: effect of wetting and capillary forces on fluid flow in heterogeneous porous media.

- o Capillary forces need to be accounted for in reservoir models and simulators.

Acknowledgement

All BS and MS students, PhD and Post.Docs, and staff, contributed with their individual research projects for more than 15 years building new knowledge, and to all project partners and the University of Stavanger for funding.

Contribution of geosciences in the exploration, preservation and heritage protection of a Mycenaean cemetery in Aidonia, Greece

Ivan Gutierrez[1], Lisa Watson[1] and Wiktor Weibull[1]

1. Department of Energy Resources, University of Stavanger

Introduction

Mycenaean Greece flourished during the Late Bronze Age from ca. 1600 BCE and declined ca. 1200 BCE (Castleden, 2005). Ten kilometers northwest from New Nemea, a Mycenaean cemetery was discovered in the Aidonia village in the mid-1970s (Fig. 1). The Aidonia tombs were dug into a hillside in the natural rock formation that are Cenozoic layers of calcareous white marlstones.

About twenty-nine Mycenaean tombs have been uncovered and excavated by archaeologists. Field observations in Aidonia revealed roofs of tombs had collapsed (Fig. 2). The cause of collapse is unknown and is a main motivation for this study.

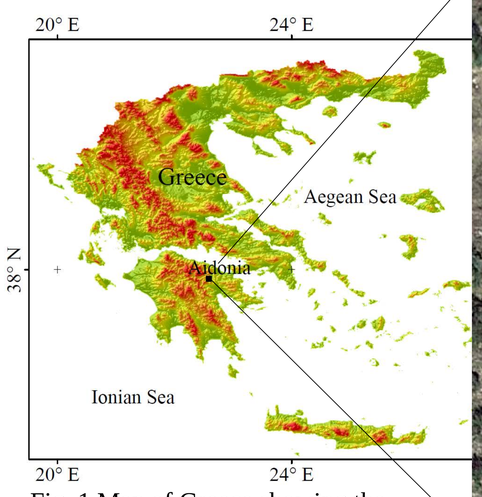

Fig. 1 Map of Greece showing the location of the Mycenaean cemetery in Aidonia.

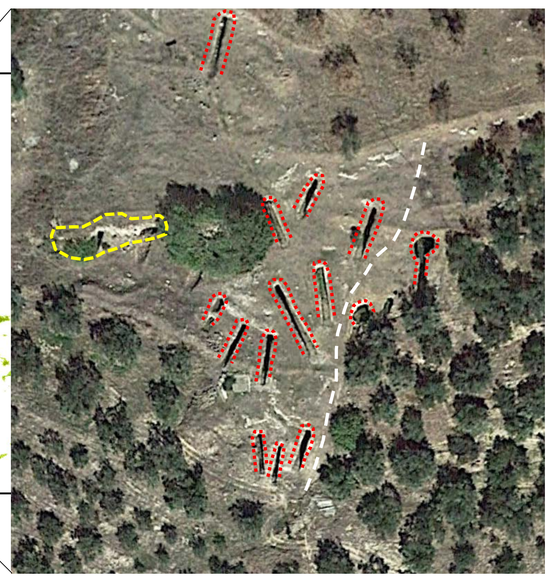

Fig. 2 Google Earth imagery showing the Aidonia Cemetery. Collapsed tombs at the right of the dashed white line. Yellow line highlights plundered tombs.

Objective

The main objective is to apply methods traditionally used in the geosciences to determine the geological process(es) (structural, sedimentological, stratigraphic, or a combination of these) responsible for collapsed Mycenaean chamber tombs.

Methods

Light Detection And Ranging (LIDAR)

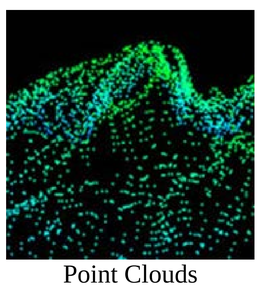

Point Clouds

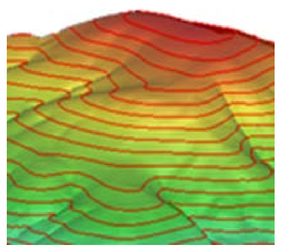

Digital Terrain Model (DTM)

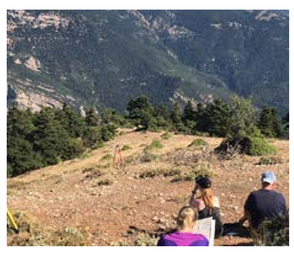

Geological Field Mapping

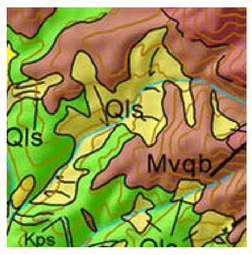

Geological Map draped onto DTM

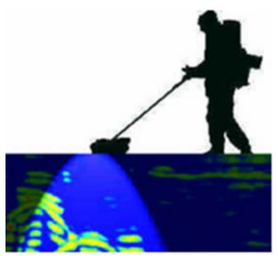

Ground-penetrating Radar (GPR). Design Solution - UAE

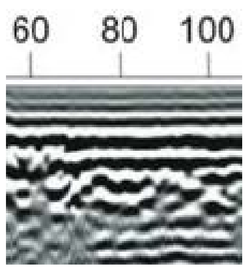

GPR Profile

Methodology

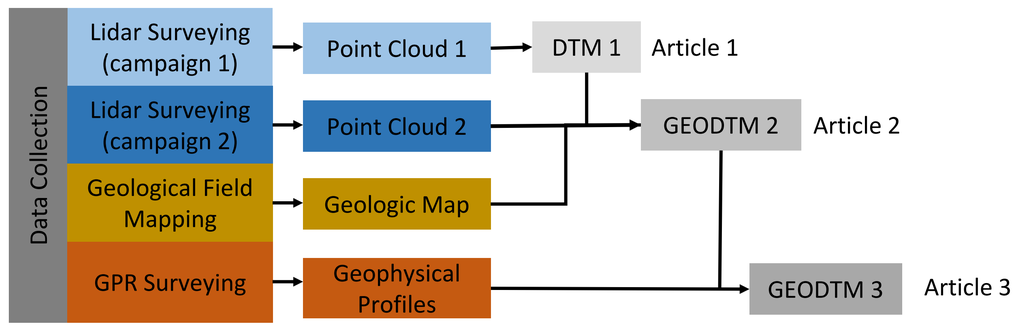

Article 1: What is the architecture and design of the chamber tombs and cemetery?

Article 2: What surficial geologic units and structures are present, and can they explain the collapse?

Article 3: What subsurface sedimentological and structural features are identified, and can they explain the collapse?

Preliminary Results

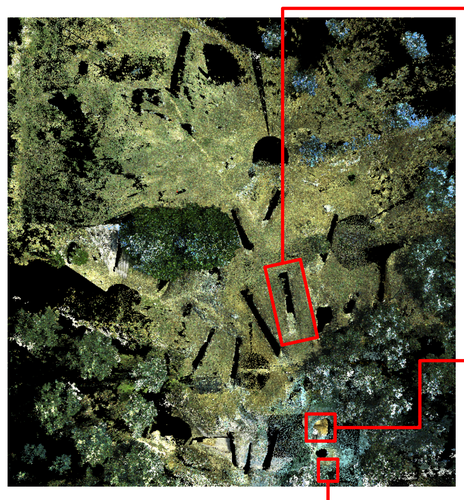

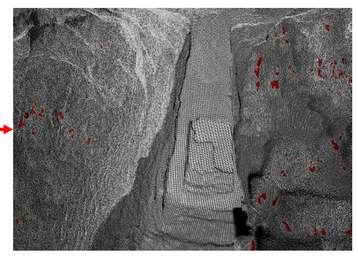

Reflectance

True Colors

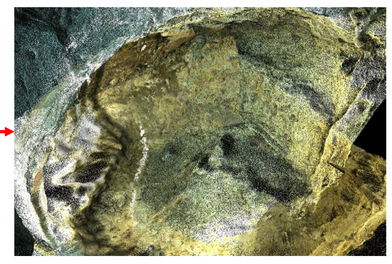

True Colors

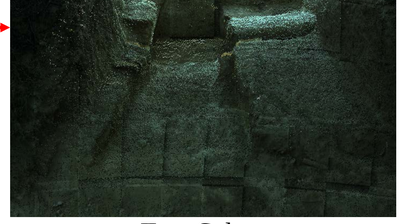

True Colors

Lidar and GPR Case Studies

LiDAR point cloud from the Oukaimeden outcrops showing interpreted stratal surfaces. Rarity et al., 2014

Georadar detection of a Viking ship in Gjellstad, Norway. NIKU

Further work

- Create a DTM model from terrestrial Lidar point clouds,
- Create a geologic field map,
- Create sub-surface geophysical profiles using ground-penetrating radar (GPR), and
- Integrate the DTM model, geologic field map, and geophysical profiles to generate a high resolution, photo-realistic, and geologically-based 3D model of the Mycenaean Cemetery.

References

Castleden, R. (2005). *The Mycenaeans*: Routledge Ltd.

Norsk institutt for kulturminneforskning. (2018). Georadar detects a Viking ship in Norway. Retrieved 2018.10.16, 2018, from https://niku.no/en/2018/10/georadar-detects-a-viking-ship-in-norway/

Rarity, F., van Lanen, X. M. T., Hodgetts, D., Gawthorpe, R. L., Wilson, P., Fabuel-Perez, I., . . . Good, T. (2013). Lidar-based digital outcrops for sedimentological analysis; workflows and techniques. *Special Publication - Geological Society of London, 387*(1), 153-183. doi:10.1144/SP387.5

The influence of salt tectonics on Mesozoic sedimentation, Norwegian Barents Sea

Luis Alberto Rojo[1], Nestor Cardozo[1], Alejandro Escalona[1], and Hemin Koyi[2]

1 : Department of Energy Resources, University of Stavanger, 4036 Stavanger, Norway
2 : Department of Earth Sciences, Uppsala University, 75236, Sweden

INTRODUCTION

Salt-bearing basins in the Barents Sea such as the Tromsø, Nordkapp, and Tiddlybanken Basins have been attractive areas for petroleum exploration from the early 80's to the present. Several exploration wells have been drilled close to salt structures in the Nordkapp Basin, proving the presence of a working petroleum system, but still no commercial discoveries have been found. As in other salt-bearing basins in the world, the occurrence of evaporitic deposits and its subsequent mobilization played an important role in the petroleum system, controlling the distribution of Triassic to Cretaceous reservoirs, influencing the style and timing of structural and stratigraphic traps, and affecting the maturation and migration of hydrocarbons (Koyi et al., 1995; Rowan and Lindsø, 2017; Gernigon et al., 2018; Rojo and Escalona, 2018; Rojo et al., 2019). Therefore, understanding salt kinematics is essential to decipher the basin evolution and improve the prospectivity of salt-bearing basins. In order to expand previous research in salt tectonics, the University of Stavanger (UIS) in collaboration with Uppsala University, currently runs a four-years R&D project (2016-2020) covering regional to prospect scale studies in salt-bearing basins located in the Norwegian Barents Sea. The project implements a multidisciplinary approach combining seismic and well interpretations, 2D/3D structural restorations, analogue modelling, and forward stratigraphic modelling to build a 4D tectono-stratigraphic evolution of salt-bearing basins located in the Barents Sea, as well as to assess the impact of salt mobilization in the petroleum system. Our results have implications for understanding the evolution and prospectivity of the salt-bearing basins of the Barents Sea and similar salt-bearing basins in the world.

REGIONAL STUDIES OF SALT-RELATED BASINS

WELL CORRELATION AND REGIONAL MAPPING

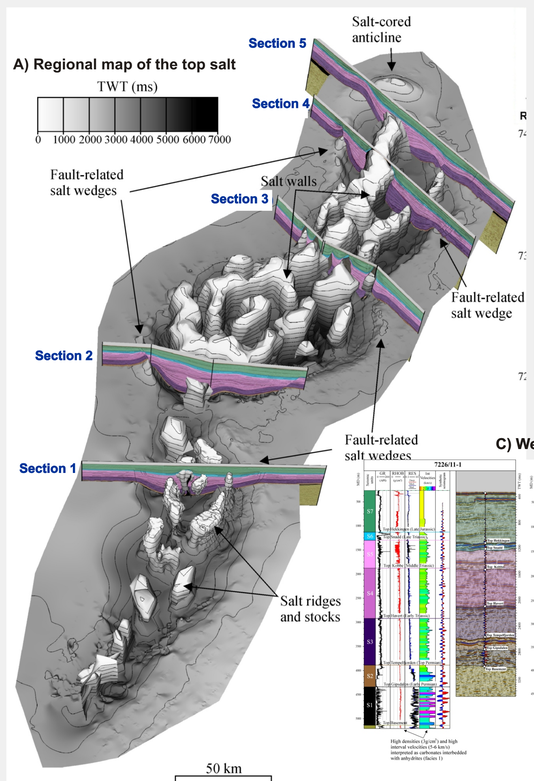

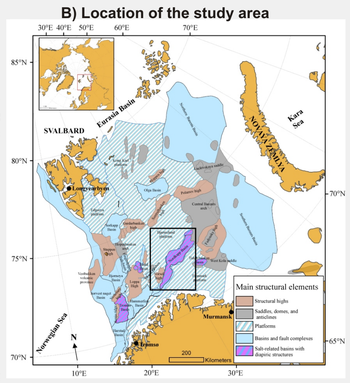

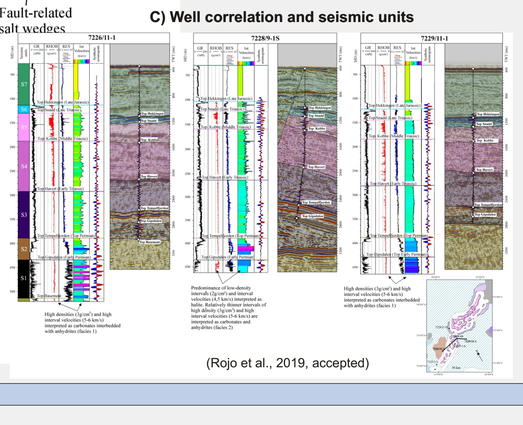

(Rojo et al., 2019, accepted)

SALT RHEOLOGY

Lithological variations of the Gipsdalen Gp based on seismic and well data

SF	Examples of seismic facies	Seismic reflection characteristics	Log response	Core example	Interpretation
F1	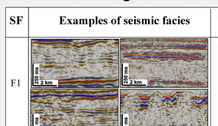	Intervals bounded at the top and base by continuous and high-amplitude seismic events. Internally, these intervals are characterized by semicontinuous, low-amplitude seismic events with locally distributed high-amplitude seismic events. In some of the sections downlap strata terminations and mound-like shapes can be recognized	- General density value (RHOB) of 3 g/cm³ - Blocky intervals of high resistivity which coincide with very high velocities (6 km/s)	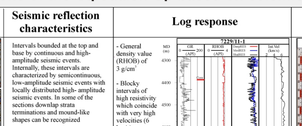	Non-mobile LES Mostly carbonate and anhydrite-dominated successions with local intervals of halite and organic-rich micritic carbonates. These sequences are interpreted to be deposited in stable platforms with presence of lagoons which become periodically isolated from oceanic waters. These sequences generally undergo minor to no halokinesis.
F2	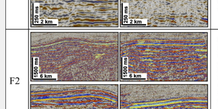	Intervals delimited at top and base by very high and continuos seismic events that laterally converge and pinch-out. Internally, these intervals are characterized by semicontinuous to chaotic, low-amplitude seismic events. Very high-seismic events often display isoclinal folding. These successions can reach up to 2000 ms	- Alternance of intervals of high density (3 g/cm³)and low density (2 g/cm³)	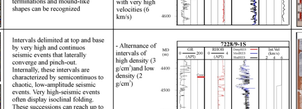	Highly-mobile LES Superposed halite-rich successions layered with carbonates, anhydrites, and organic-rich mudstones, which appear deformed due to halite mobilization. These sequences are interpreted as basinwide evaporites deposited in tectonically isolated basins from oceanic waters. Basin wide evaporites can reach up to several km. The large amount of halite-rich sequences could favour halokinesis and diapir growth.

SEISMIC VS ANALOGUE MODELS

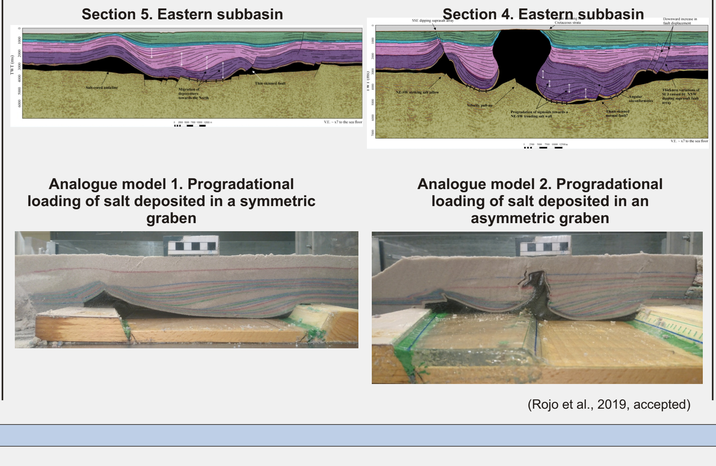

(Rojo et al., 2019, accepted)

4D TECTONO-STRATIGRAPHIC EVOLUTION

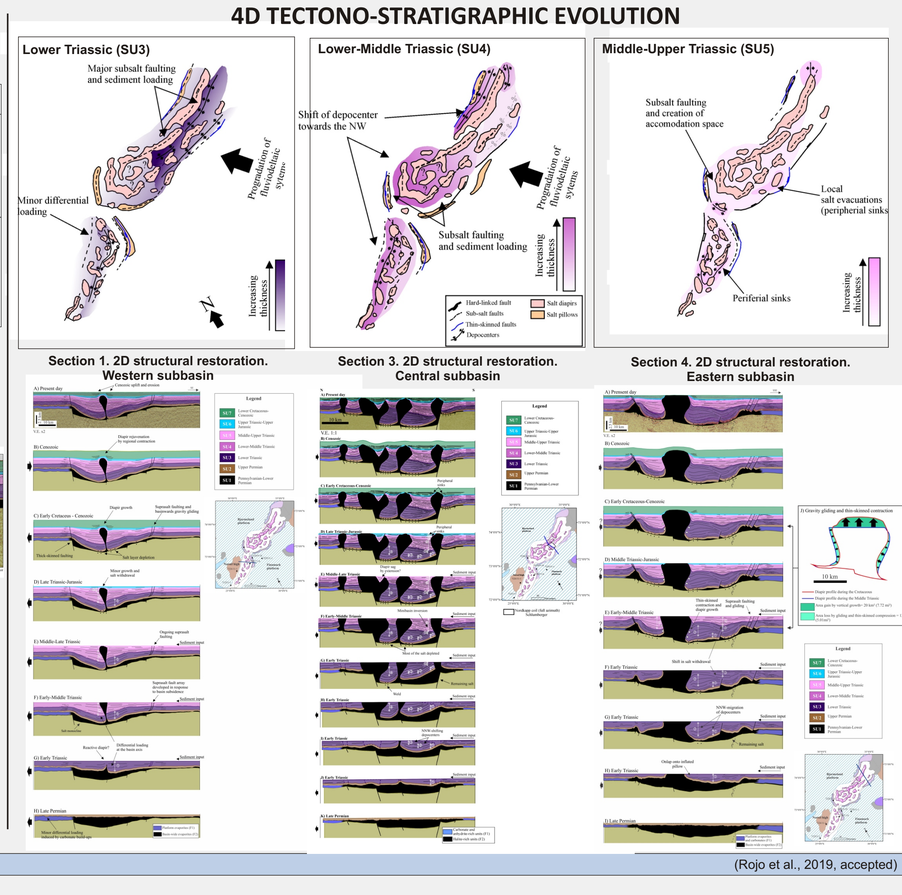

(Rojo et al., 2019, accepted)

NEAR-DIAPIR DEFORMATION AND MINIBASIN INFILL

Core and well log interpretation from well 7228/7-1A drilled in a salt minibasin

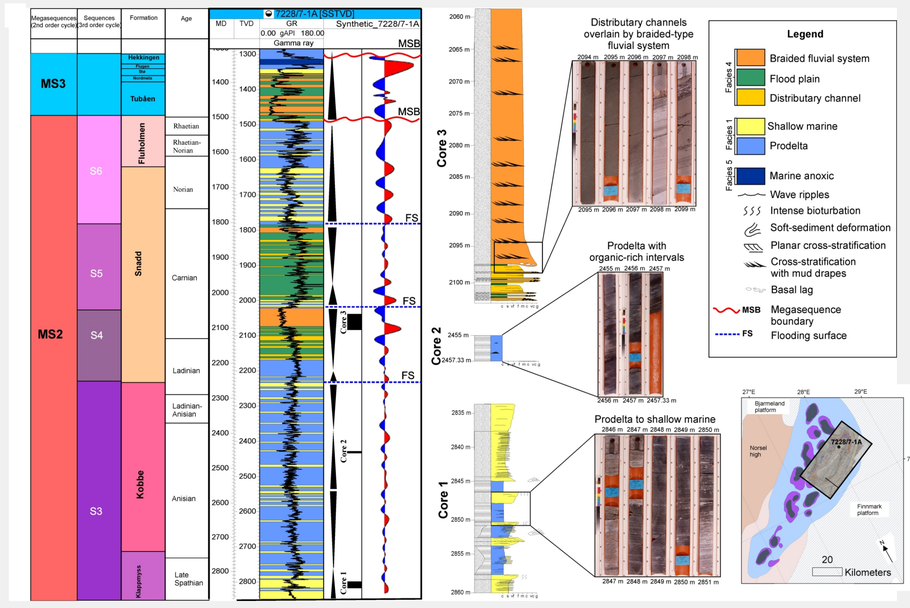

(Rojo and Escalona, 2018)

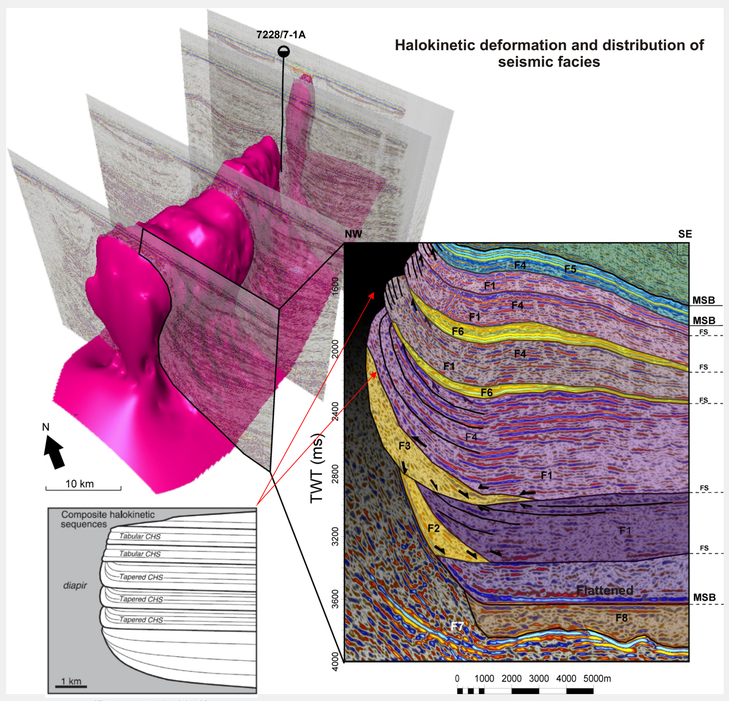

(Rowan et al., 2016)

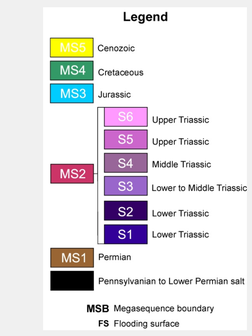

(Rojo and Escalona, 2018)

Conceptual models of Mid-Late Triassic minibasin infill

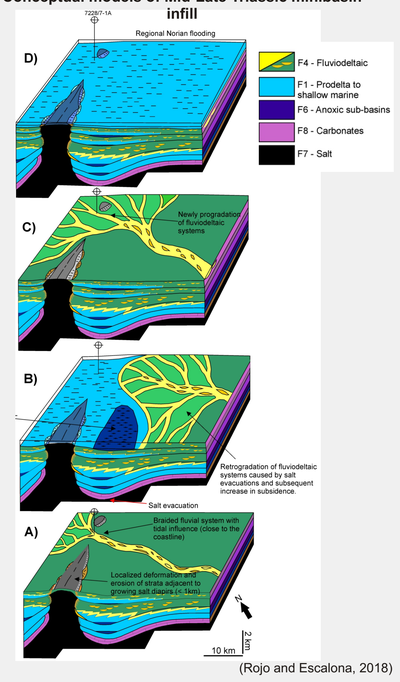

(Rojo and Escalona, 2018)

THE INFLUENCE OF HALOKINESIS IN PROGRADING OVERBURDENS

Lateral variations in clinoform geometry and trajectory along the Tiddlybanken Basin

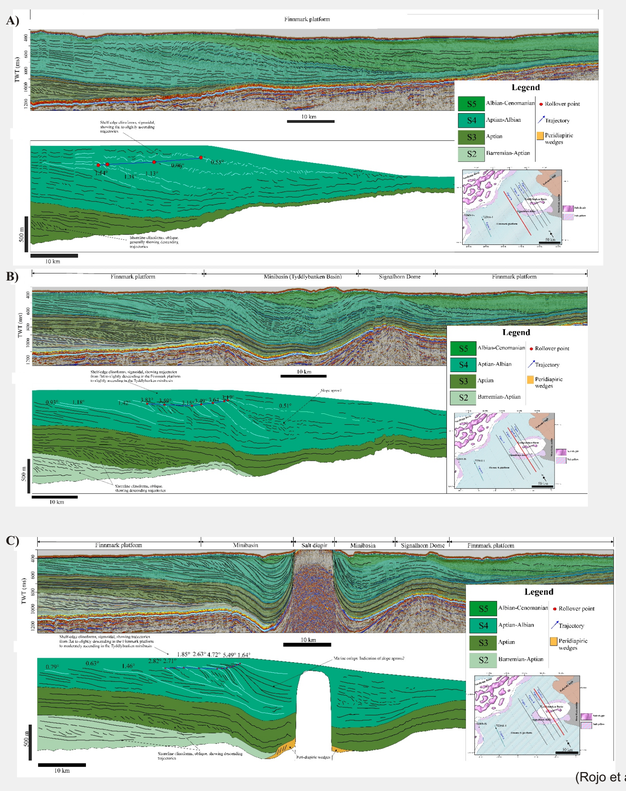

3D-structural restoration of the Tiddlybanken Basin during the Early Cretaceous

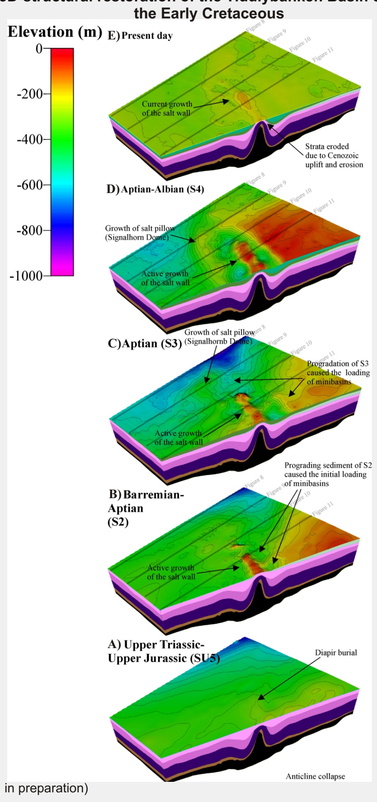

Forward stratigraphic modeling of shelf-edge clinoforms prograding through the Tiddlybanken Basin

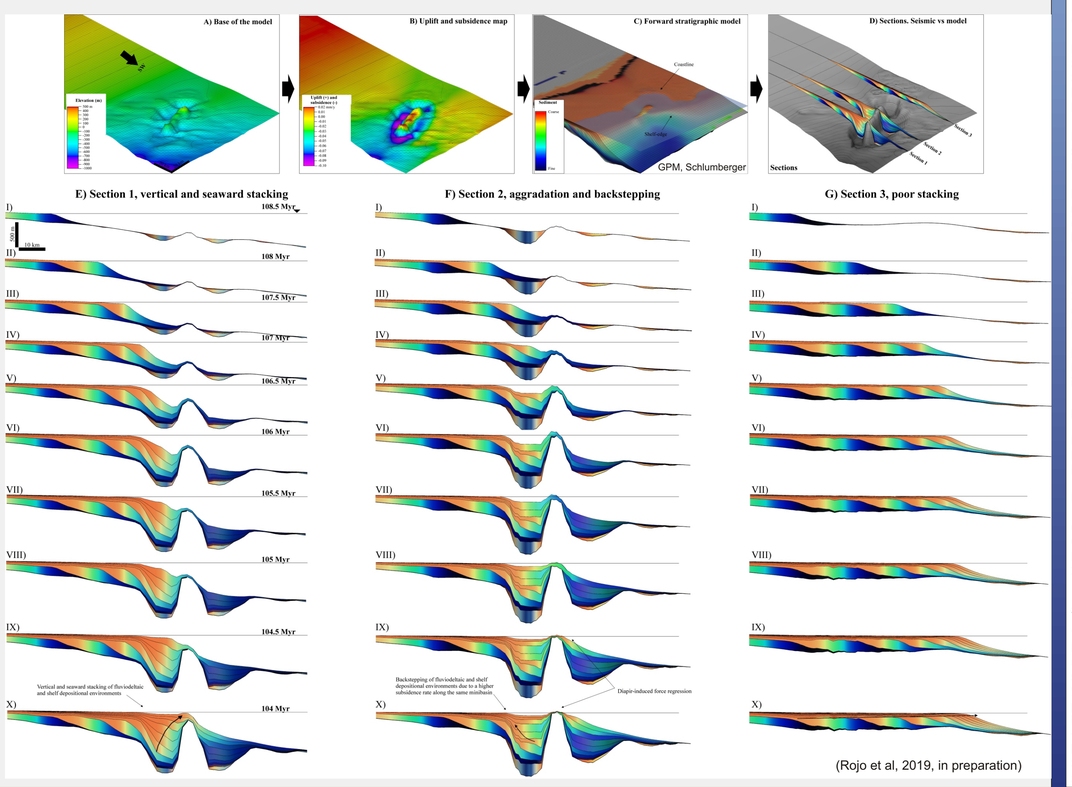

(Rojo et al, 2019, in preparation)

(Rojo et al, 2019, in preparation)

References

Gernigon, L., M. Brönner, M.-A. Dumais, S. Gradmann, A. Grønlie, A. Nasuti, and D. Roberts, 2018, Basement inheritance and salt structures in the SE Barents Sea: Insights from new potential field data: Journal of Geodynamics

Koyi, H., C. J. Talbot, and B. O. Tørudbakken, 1995b, Salt tectonics in the Northeastern Nordkapp basin, Southwestern Barents sea, in M. P. A. Jackson, D. G. Roberts, and S. Snelson, eds., Salt Tectonics: A Global Perspective, AAPG Memoir 65, p. 437-447

Rojo, L.A., A. Escalona, and L. Schulte, The use of seismic attributes to enhance imaging of salt structures in the Barents Sea: First Break, V. 34, NO. 11, p. 49-57.

Rojo, L. A., and A. Escalona, 2018, Controls on minibasin infill in the Nordkapp Basin: Evidence of complex Triassic synsedimentary deposition influenced by salt tectonics: AAPG Bulletin, V. 102, NO.7, p. 1239-1272.

Rojo, L. A., N. Cardozo, A. Escalona, and H. Koyi, 2019, Tectonostratigraphic evolution and structural style of the Nordkapp Basin, Norwegian Barents Sea: AAPG Bulletin, accepted.

Rojo, L.A., D. Marin, N. Cardozo, A. Escalona, and H. Koyi, 2019, in preparation, The influence of halokinesis in prograding overburdens: insights from the Tiddlybanken Basin, Norwegian Barents sea, in preparation.

Rowan, M. G., K. A. Giles, T. E. Hearon IV, and J. C. Fiduk, 2016, Megaflaps adjacent to salt diapirs: AAPG Bulletin, v. 100, p. 1723-1747.

Rowan, M. G., and S. Lindsø, 2017, Chapter 12 - Salt Tectonics of the Norwegian Barents Sea and Northeast Greenland Shelf A2 - Soto, Juan I, in J. F. Flinch, and G. Tari, eds., Permo-Triassic Salt Provinces of Europe, North Africa and the Atlantic Margins, Elsevier, p. 265-286.

Acknowledgements

We acknowledge the Norwegian Petroleum Directorate for giving us access to the DISKOS database and for kindly providing the NPD-BA-11 2D seismic survey in the eastern Norwegian Barents Sea. We acknowledge WesternGeco Multiclient for providing wide azimuth 3D seismic data from the Nordkapp Basin to the University of Stavanger. We are very grateful to the GPM team in Schlumberger for its help and support with the software. Thanks to Schlumberger and Midland Valley for providing academic licenses of their softwares Petrel and Move.

Control of Upper Jurassic submarine fan systems by oblique-slip transfer faults in segmented rift systems: Evidence from the southern margin of the Sogn Graben, northern North Sea

Xiaoan Zhong, Alejandro Escalona, Carita Augustsson

Department of Energy Resources, University of Stavanger

Author contact: xiaoan.zhong@uis.no

Introduction

In passive margins, rift systems can be segmented along the axis by transfer zones/faults. Few works have discussed how transfer faults have the potential to modify the pattern of drainage systems and therefore determine the architecture of the different depositional systems.

This study focuses on the Upper Jurassic rift system in the southern Sogn Graben aiming to explain how the submarine fan systems were controlled by syn-depositional normal faults and transfer faults.

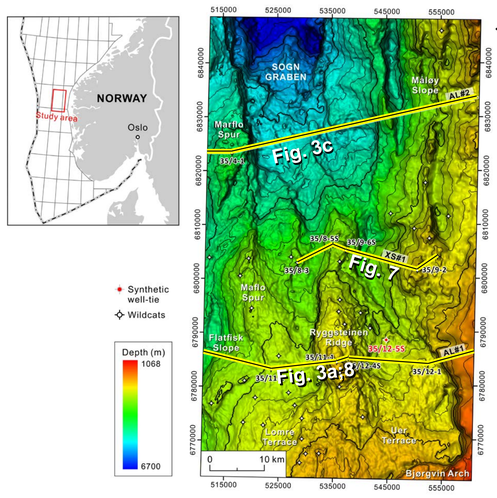

Fig. 1 Location map of the study area. The base grid is along the Basal Cretaceous Unconformity.

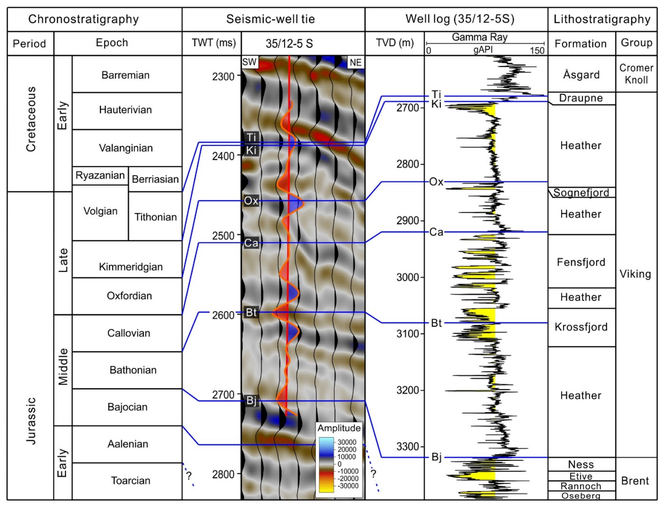

Fig. 2 Regional stratigraphy and synthetic seismic-well tie

Structural framework

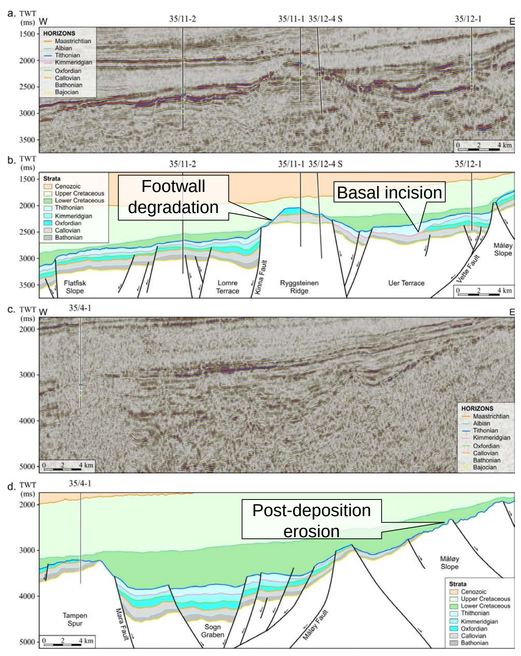

Fig. 3 Traverse seismic lines

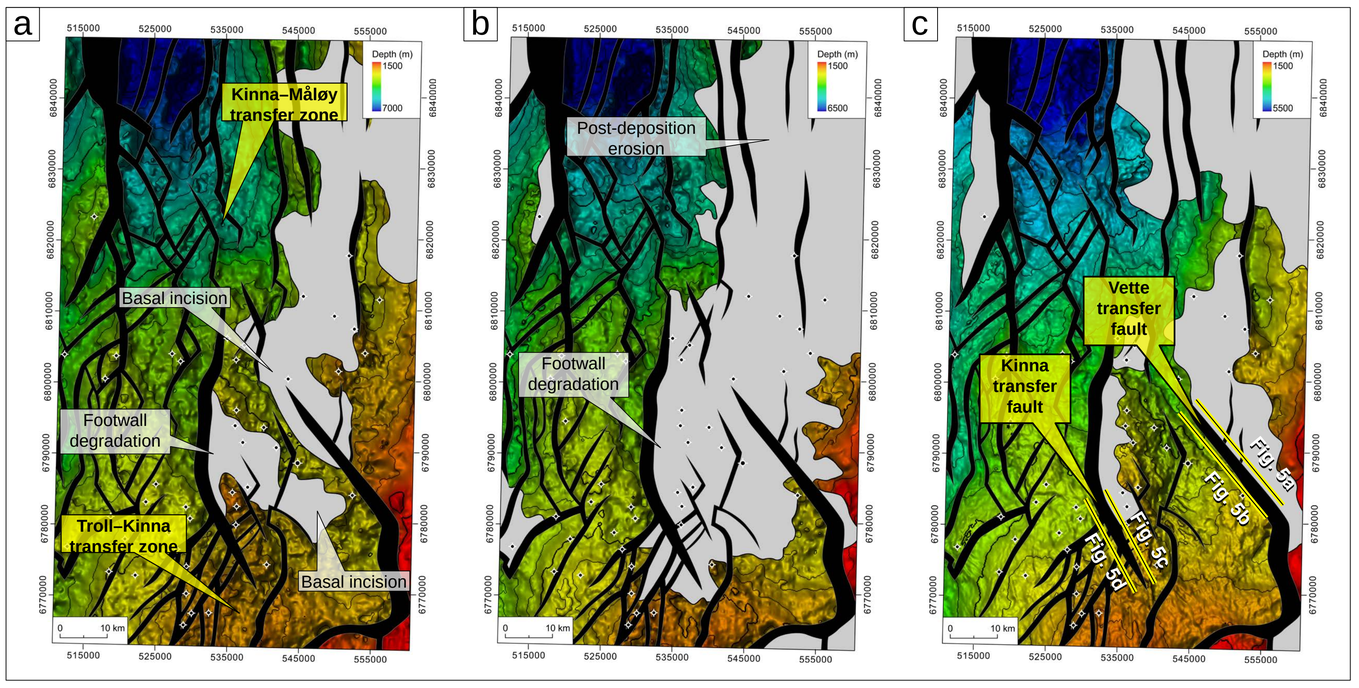

▲ Fig. 4 Structural maps at the tops of Oxfordian (a), Kimmeridgian (b), and Tithonian(c)

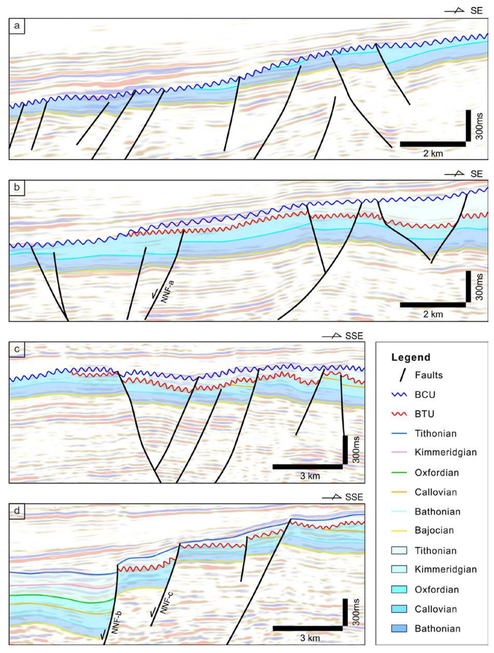

▲ Fig. 5 Strike-parallel seismic profiles showing the minor faults in transfer fault blocks

Facies association defined from conventional cores

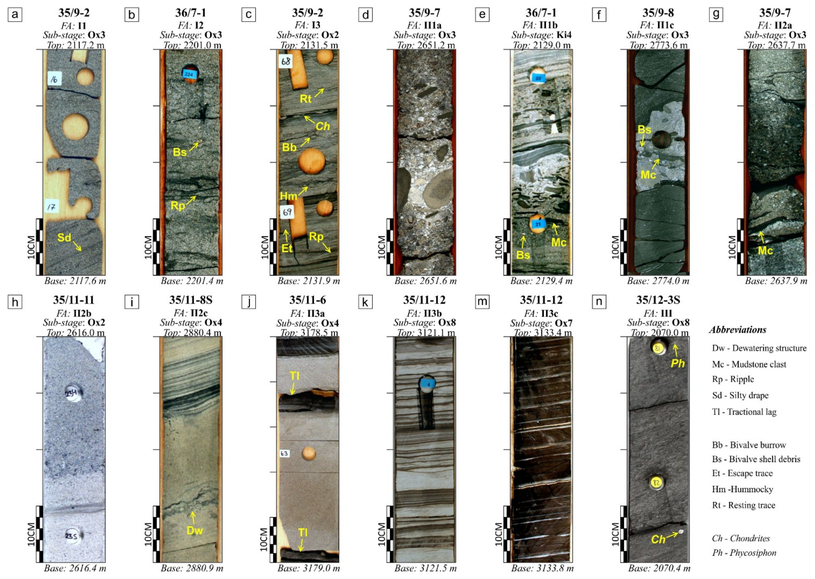

▲ Fig. 6 Shoreface (a-c) and sandy gravity flow deposits (e-n)

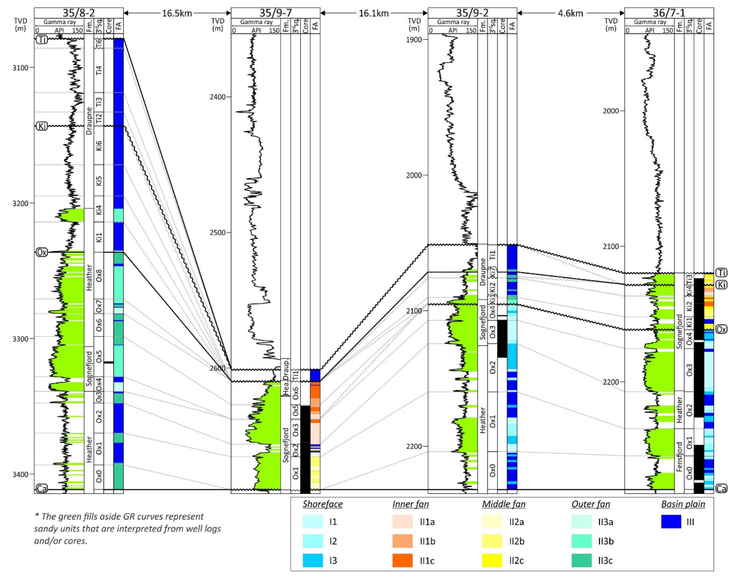

▲ Fig. 7 Facies associations in the northern section

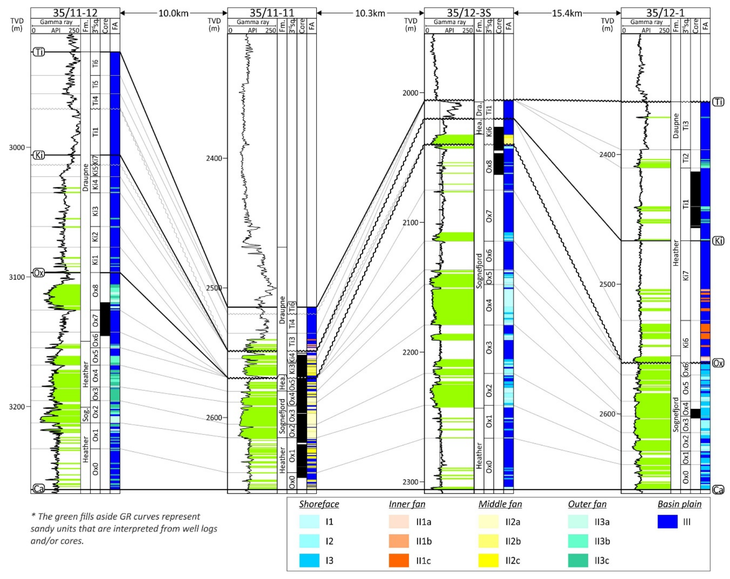

▲ Fig. 8 Facies associations in the southern section

Paleo-geography reconstruction

Fig. 9 Evolution of faults and the syn-rift depositional system

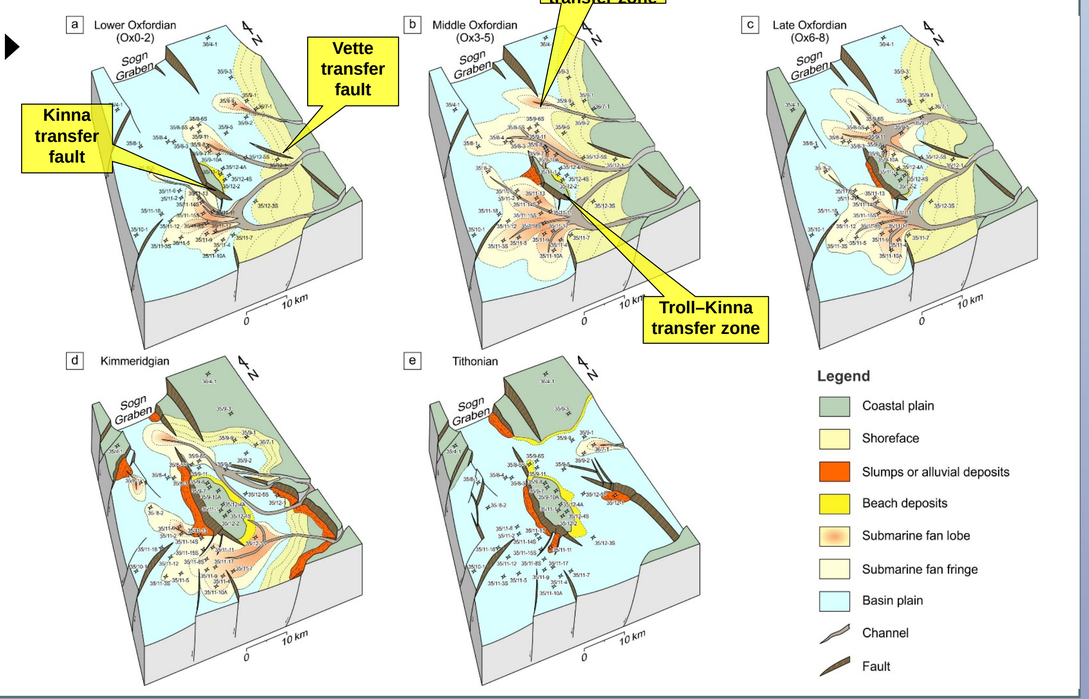

a – Lower Oxfordian

b – Middle Oxfordian

c – Upper Oxfordian

d – Kimmeridgian

e - Tithonian

Conclusion

- The Upper Jurassic rift system was segmented by the offset of longitudinal normal faults and NW–SE-striking transfer faults with dextral oblique-slip motion.
- The submarine fan systems comprise debris-flow-dominated channels and turbidity-flow-dominated lobe complexes, and are occasionally mixed with slump deposits.
- The development of Upper Jurassic submarine fans was controlled by transfer faults in segmented rift system in the southern Sogn Graben.

Acknowledgement

This research is sponsored by Spirit Energy.

Department of Energy Resources Research Day 2018

Study on Value of Perfect Information of 4D Seismic Surveys Using Ensemble Assimilation Methods

Camilo Malagon Nieto. PhD Candidate

Advisor: Reidar Bratvold, Professor UiS

Co-advisor Remus Hanea, Associate Professor UiS

University of Stavanger

Introduction

4D Seismic is an important source of information for field development optimization and maximizing NPV. It allows:

Recognition of :	**Revaluation of :**
- Aquifer encroachment - Undrained areas - Aquifer fronts - Reservoir compartmentalization	- Development plan - Alteration of development drilling program - Addition of new wells - Changes on the injection/production schedule

To estimate the cost/benefit of implementing a GRM (Geophysical Reservoir Monitoring) method poses several challenges.

- How to assess the potential benefit of a future measurement?
- How to estimate the future actions upon survey results?

Assessment performed by a heuristic estimation based on technical constraints rather than economic optimum valuation.

Objective

- Simulate reservoir management decision of investing or on a 4D seismic acquisition for a simple synthetic case.
- Test viability of Closed Loop Reservoir Management (CLRM) for decision analysis studies of Value of Information (VoPI) through use of robust optimization and data assimilation.

Method

A reservoir management simulation (RM-Sim) along the life of the asset is performed using the CLRM workflow in order to observe the difference of net present value with and without the use of 4D seismic interpreted as a saturation values.

Close Loop Reservoir Management CLRM

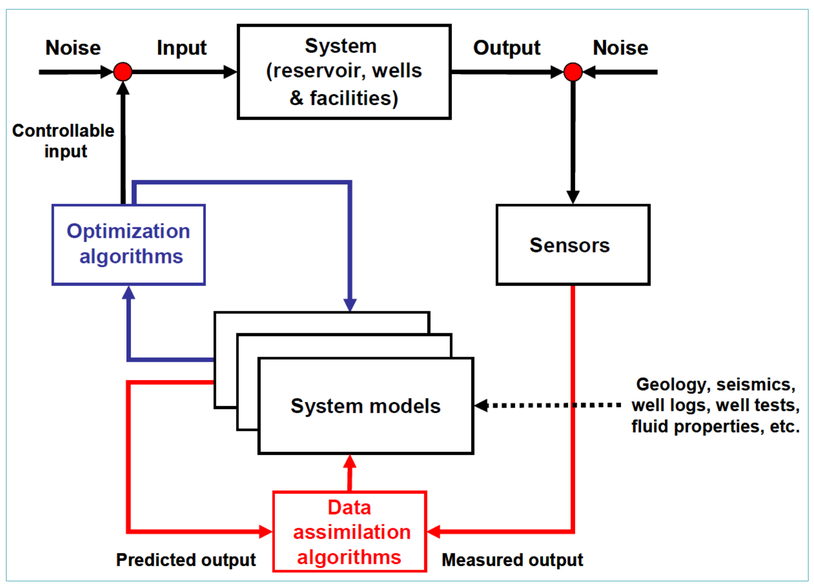

SPE 119098 Closed-Loop Reservoir Management, Jansen, et. al. 2009

1. Simple synthetic reservoir is created.
2. Uncertainty simulated with 100 members' ensemble
3. Genetic Algorithm emulates well schedule decisions.
4. ES-MDA assimilation of production/Seismic data (WSat).
5. VOPI = EV(with perfect information) – EV (original deal)

Simulation Workflow

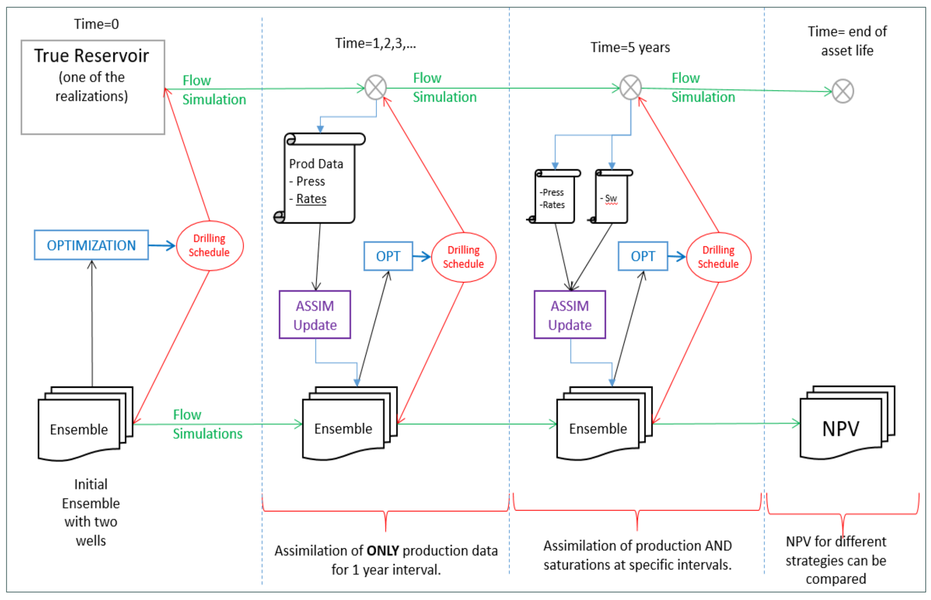

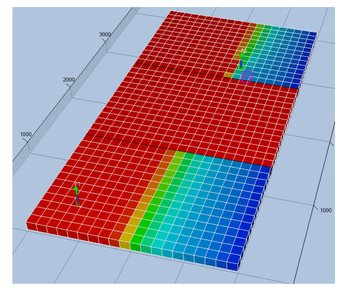

- Simple 2D Model
  - Based on SPE3 black oil model.
  - Strong compartmentalization case.
  - Starts with only two discovery wells.
- Model Uncertainties
  - Assumes fault's transmissibility unknown
  - Porosity and Permeability unknown.
- Model REMA
  - 20X40x1 cells wih size 100x100x20 ft
  - Two phase system with oil and water
  - Fault sealing from north/west/south
  - Strong aquifer influx from east

Robust Optimization / Genetic Algorithm

Global optimization of well locations for 7 development wells.
Objective function = NPV

10% elite	50 gene population
20 % crossover	5-10 generations
70% mutation	100 ensemble

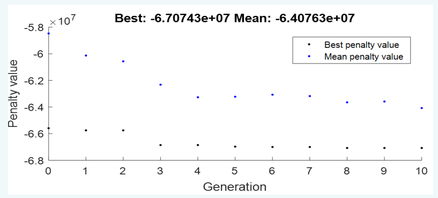

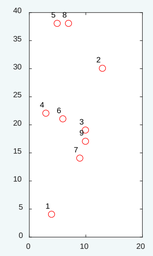

Data Assimilation / ES-MDA

Ensemble Smoother with Multiple Data Assimilation.

$$\mathbf{m}_j^{\ell+1} = \mathbf{m}_j^{\ell} + \mathbf{C}_{\mathbf{MD}}^{\ell}\left(\mathbf{C}_{\mathbf{DD}}^{\ell} + \alpha_\ell \mathbf{C}_{\mathbf{D}}\right)^{-1}\left(\mathbf{d}_{\mathrm{pert,j}} - \mathbf{d}_j^{\ell}\right)$$

$$\sum_{\ell=1}^{N_a} \frac{1}{\alpha_\ell} = 1$$

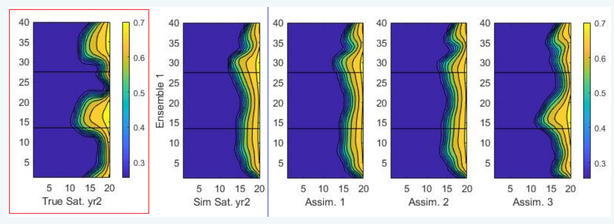

Example of 8 Year of Optimization/Assimilation

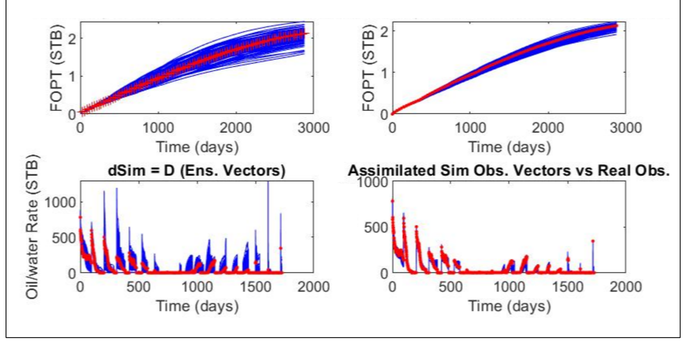

Full Scale VOPI simulation Proposed Schedule

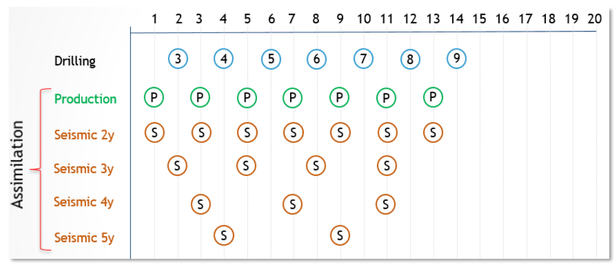

Conclusion

- Study presents implementation of Closed Loop Reservoir Management workflow to estimate Value of Information(*) for 4D seismic acquisitions.
- A sequence of Optimization/Assimilation allows a decision maker to assess 4D seismic investment under geologic uncertainty.
- The workflow present a robust alternative to the traditional expert assessment.

Further Work

- Deployed workflow will serve as a decision analysis modeling tool to assess VOI with imperfect information and further study when the reservoir is unknown.
- Addition of synthetic seismic simulation and inversion to assess imperfect information surveys.
- Workflow can include value of flexibility studies, optimization of seismic installations (Resolution/Quality), evaluation of technical requirements, Comparison between Survey methods.

Acknowledgement

- Department of Energy and Petroleum Engineering UiS
- Javad Rafiee, University of Tulsa

NUMERICAL MODELLING OF NON-DARCY FLOW IN SHALE GAS PRODUCTION

Temidayo O. Boboye[2], Dhruvit S. Berawala[1,3], Pål Ø. Andersen[2,3], Zhixin Yu[1,3]

1. Department of Energy and Petroleum Technology, University of Stavanger
2. Department Of Energy Resources, University of Stavanger
3. The National IOR Centre of Norway

Introduction

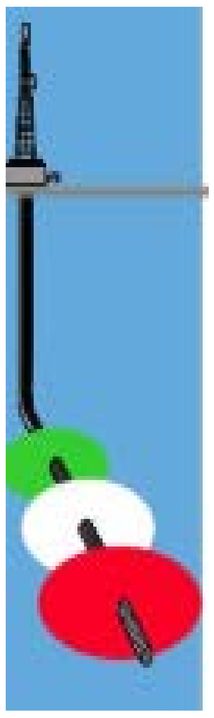

Hydraulic Fracturing (Peter P. Valko, 2005)

Shale gas reservoirs are organic rich formations and composed of free gas in micro-fractures and adsorbed gas in shale matrix. Shale reservoir has ultra-low permeability with nanopore structure. Darcy flow cannot fully describe the matrix-fracture inflow.

Non-Darcy flow mechanisms significantly affects gas recovery rates, contributing parameters includes Forchheimer term, apparent permeability, gas diffusion and desorption.

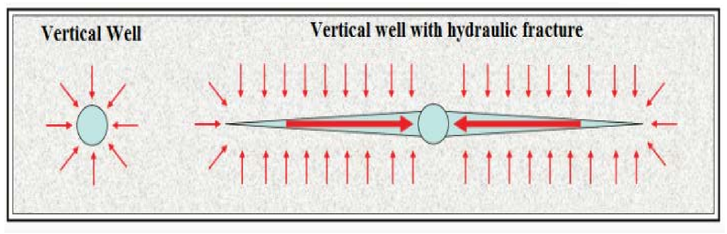

Hydraulic Fractures (Emmanuel Martins, 2017)

Objective

- To review relevant flow and storage mechanisms and modelling approaches.
- To investigate the governing parameters for transition from non-Darcy to Darcy flow, especially at the transition between fracture and matrix.
- To suggest relevant reference parameters, scaling of the model and dimensionless numbers.

Method

Extending the model presented in Berawala et al. (2018) by including non-Darcy mechanisms: Forchheimer term and apparent permeability.

Fracture domain:

$$\phi^f b(y)\partial_t(P_g) = -\left(ub(y)\partial_y P_g + \frac{P_g k_a^f}{\mu + 2\beta^f P_g k_a^f}\right) - \left(P_g u\right)_{x=0,y}$$

Matrix domain:

$$\phi^m b\,\partial_t\left(P_g + \hat{a}_{max}\frac{P_g}{P_g + P_L}\right) = -u\partial_y P_g \;-\; P_g\frac{k_a^m}{\mu_g + 2\beta^m P_g k_a^m}\frac{\partial^2 P_g}{\partial x^2}$$

Langmuir Isothermal Adsorption term

$$\hat{a}_g = \frac{1-\phi}{\phi b_g' \rho_g^s} a_g = \hat{a}_{max}\frac{P_g}{P_g + P_L}\;,\quad \hat{a}_{max} = \frac{1-\phi}{\phi b_g' \rho_g^s} a_{max}$$

$$\textit{Apparent Permeability}\quad k_a = \frac{\mu_g Z r^2}{8 P_g r_e}\sqrt{\frac{\pi RT}{2M}}$$

$$\text{Forcheimer term } \beta = \frac{4.8\times 10^{12}}{K_a{}^{1.176}}$$

K_n	$0 - 10^{-3}$	$10^{-3} - 10^{-1}$	$10^{-1} - 10^{1}$	$> 10^{1}$
Flow regimes	Continuum	Slip	Transition	Free Molecular

Fluid flow regimes defined by ranges of K_n (Roy et al. 2003)

Results

- By means of scaling, it can be shown that the behavior of shale gas production is controlled by three dimensionless numbers.
- Key parameters are identified for optimized design of perforations and well-induced fractures.
- Model validation against commercial software.
- Non-Darcy flow impacts gas production, but can be accounted for in a simple manner in the model.

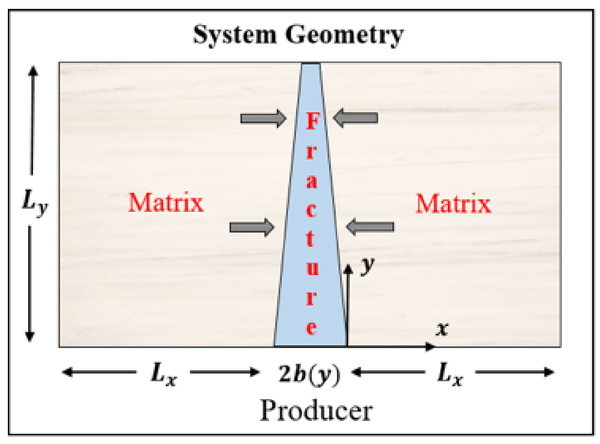

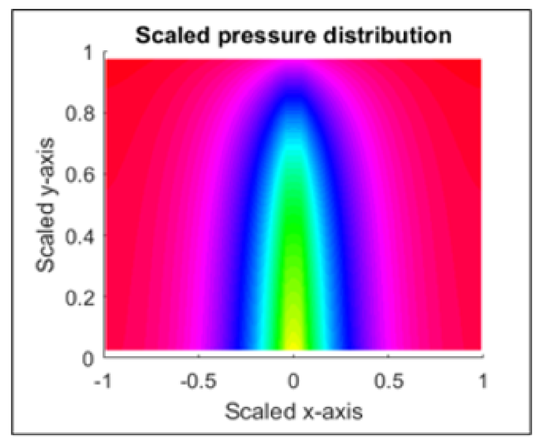

System Geometry (Berawala et al. 2018)

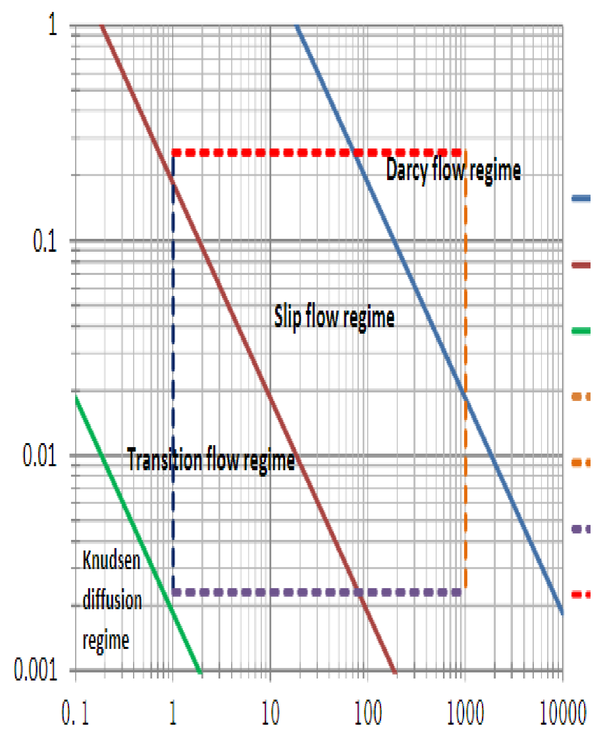

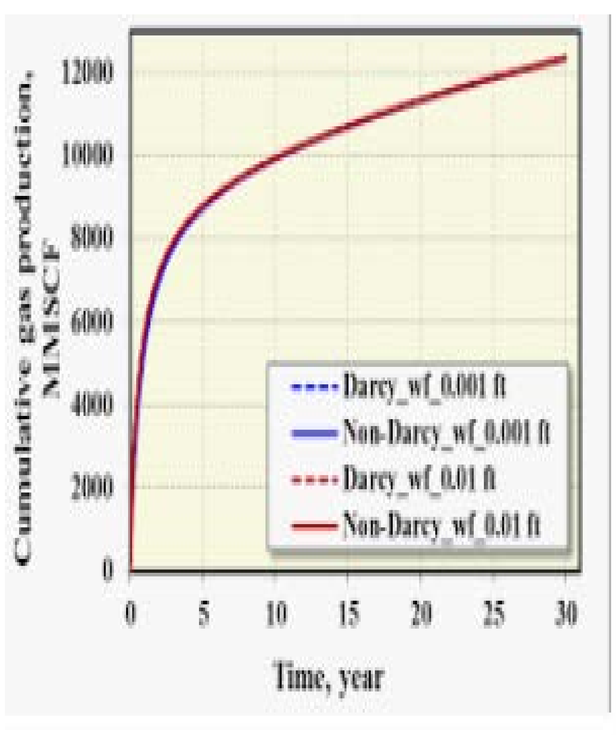

Sensitivity study & history matching & economics optimization for Marcellus Shale (W.Yu, K. Seperhrnoori, 2014)

Conclusion

The proposed 1D + 1D model is a useful tool to evaluate the sensitivity of more complex flow mechanism such as non-Darcy flow for high velocity of gas in fracture and matrix. Identifying the transition from non-Darcy to Darcy, will prevent additional pressure at wellbore.

Further work

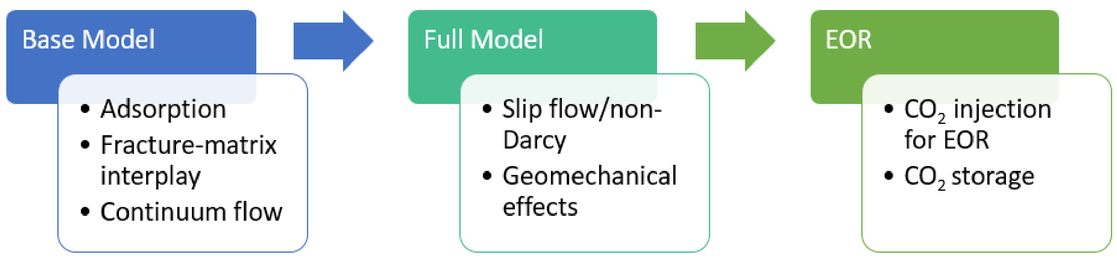

Acknowledgement

The authors acknowledge the Research Council of Norway and the industry partners, ConocoPhillips Scandinavia AS, Aker BP ASA, Eni Norge AS, Total E&P Norge AS, Equinor ASA, Neptune Energy Norge AS, Lundin Norway AS, Halliburton AS, Schlumberger Norge AS, Wintershall Norge AS, and DEA Norge AS, of The National IOR Centre of Norway for support.

Source rock variations within the Hekkingen Formation

Andres Cedeño, Sverre Ohm, and Alejandro Escalona

University of Stavanger

Introduction

Source rocks are not homogenous entities, but rather vary vertically and laterally in response to changes in depositional environments and inherent variations in primary organic material. For example, the land-derived organic matter (**type III kerogen**) may also be an important contributor to marine settings (**type II kerogen**), either in shallow marine, deltaic or open marine environments (figure 1). The former seems to be the case of the Upper Jurassic Hekkingen Formation in the Norwegian Barents Sea for which oils of different composition, reflecting variations in the primary organic matter, have been reported.

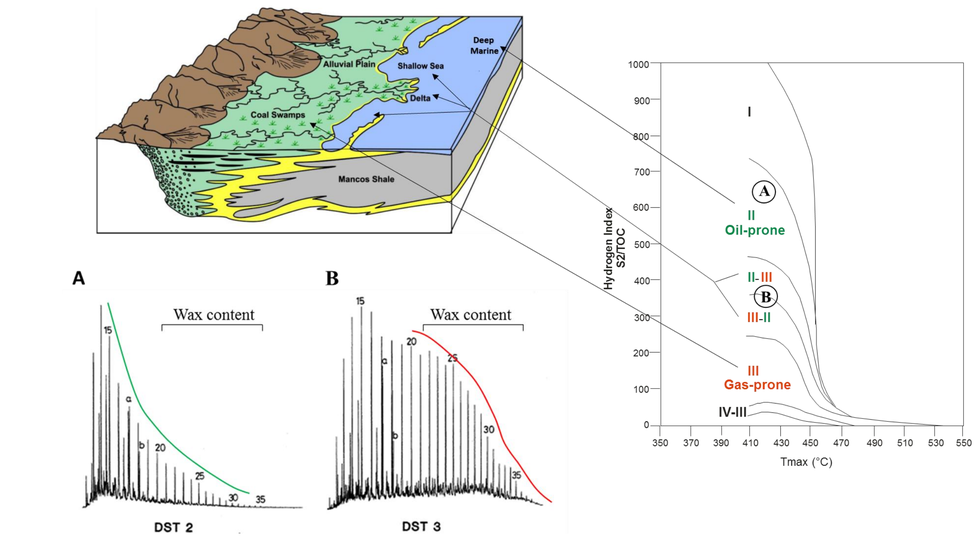

Figure 1. Diagram showing continental and marine depositional environments (left) and a Tmax vs. Hydrogen Index (HI) plot outlining Kerogen types (right). A and B represent GC-FID traces for a typical marine and terrestrial Snøhvit oils, respectively.

Objectives

To identify facies variations using different geochemical data and define gross kinetics honoring such variations in order to better understand timing and hydrocarbon phases generated.

Method

In order to identify variations in organic matter this study will include interpretation and integration of:

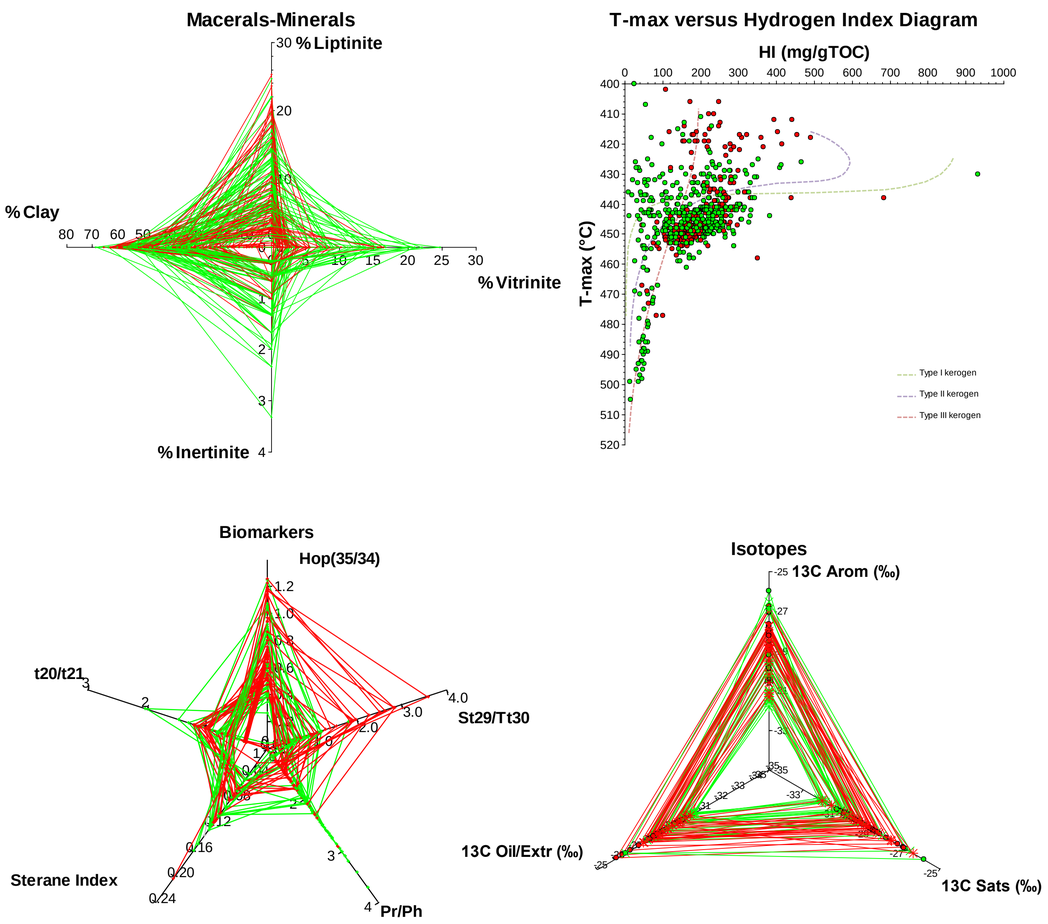

Results

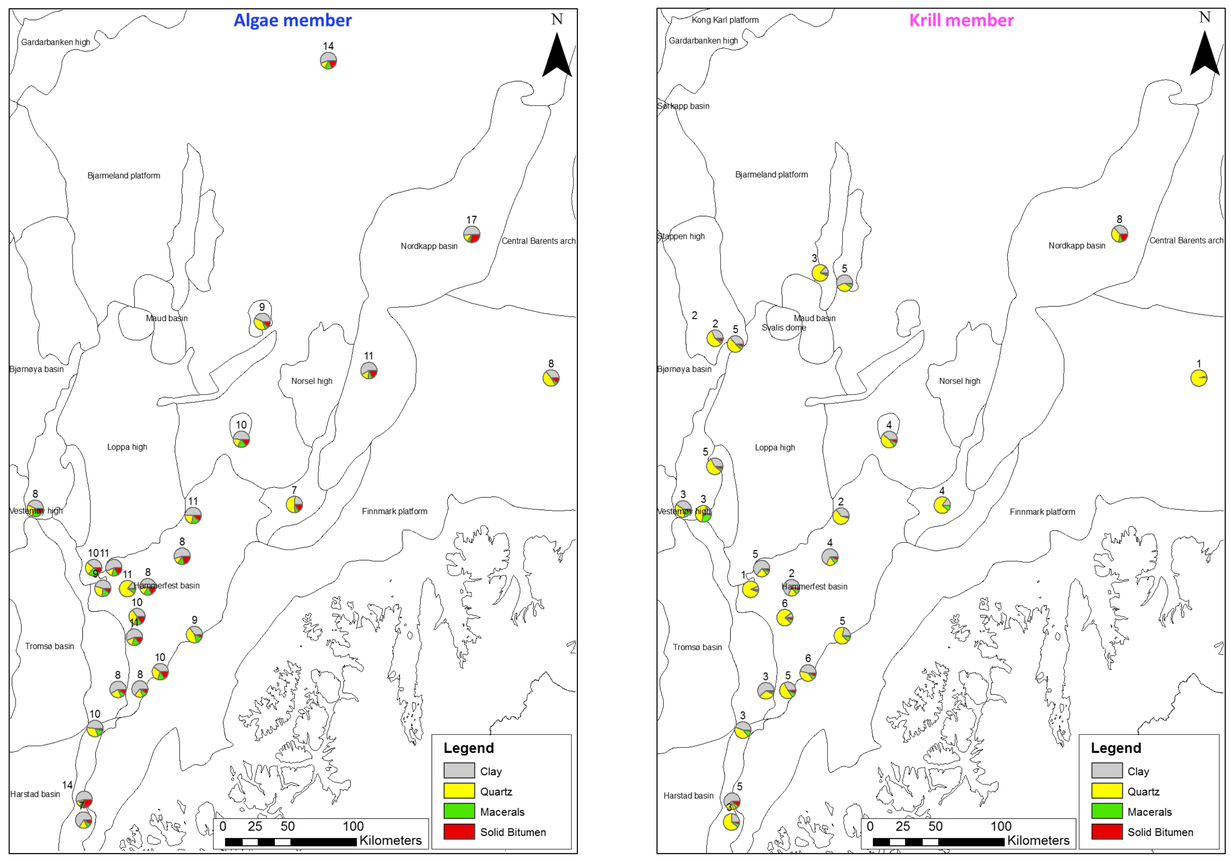

Figure 2. Maps showing average content (%) of Clay, Quartz, Macerals, and Solid Bitumen in **Algae** (left) and **Krill** (right) members at different well locations. Numbers represent average TOC values. The Algae member shows higher content of clay and solid bitumen than the Krill member. Maximum TOC values occur in the northern part of the Nordkapp basin for both members.

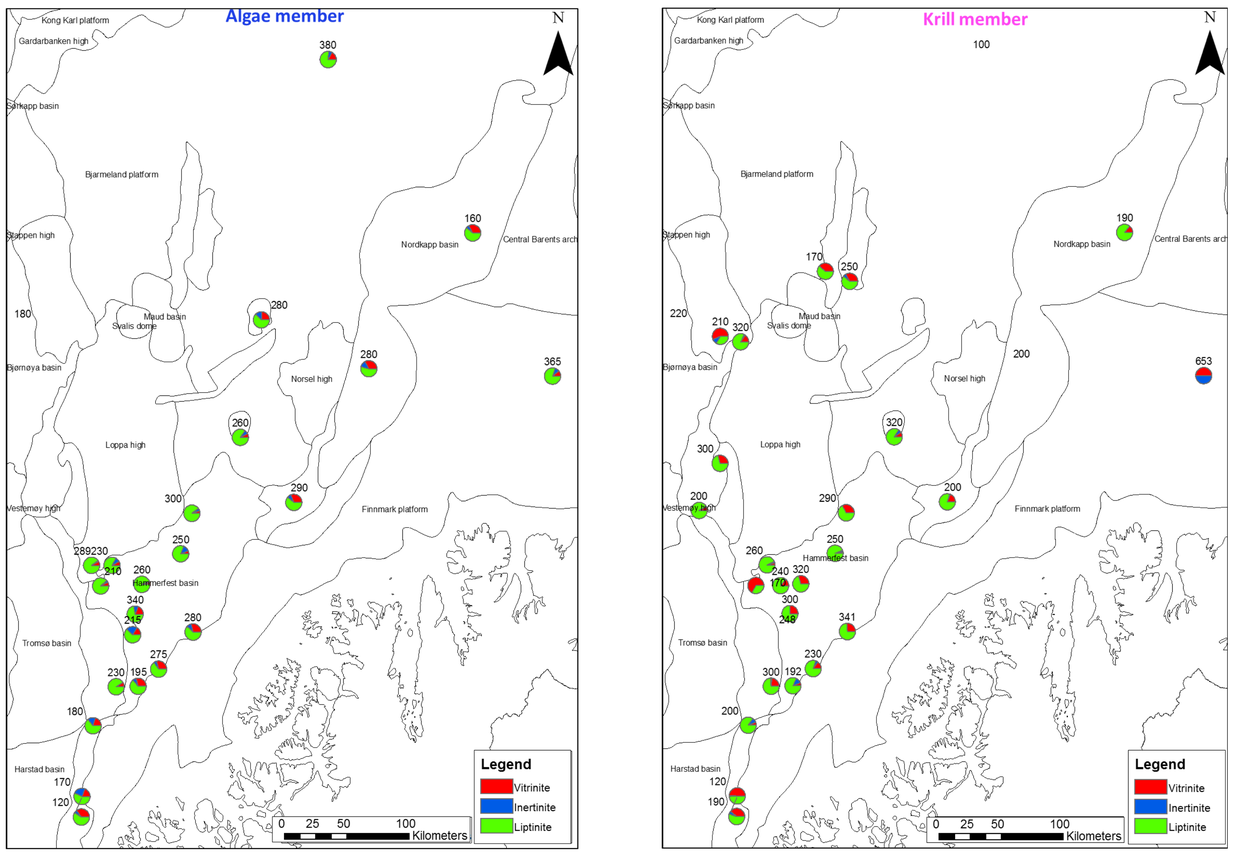

Figure 3. Maps showing average content (%) of Vitrinite, Inertinite, and Liptinite macerals in **Algae** (left) and **Krill** (right) members at different well locations. Labels represent average HI and average percentage of Macerals. Overall, the Algae member in the Hammerfest basin shows a lower amount of vitrinite relative to the Krill member. The Northern Finnmark Platform show the highest HI in the data set, while the northern portion of the Nordkapp basin shows the lowest HI.

Discussion

- ✓ At a given location, Algae and Krill can differ significantly in their HI. Likewise, variations in HI are observed laterally within the same member. Having said that, what is/are the hydrocarbon phases (oil/gas) to be expected from these members in different locations within the Barents Sea?
- ✓ The Krill member has lower TOC content, but similar HI values to those of the underlying Algae member. However, the former has comparatively higher percentage of Solid Bitumen and clay, which leads us to consider: what is the expulsion efficiency of the Algae member?

Future work

Kinetics Analysis - Basin modelling – Effect of solid bitumen in expulsion efficiency.